

EUR 4880 e

COMMISSION OF THE EUROPEAN COMMUNITIES

**RAPID DEPRESSURIZATION OF A THERMAL
INSULATION SYSTEM FOR HIGH TEMPERATURE
GAS REACTORS**

by

E. ARANOVITCH and D. VAN ASSELT

1972



**Joint Nuclear Research Centre
Ispra Establishment - Italy**

LEGAL NOTICE

This document was prepared under the sponsorship of the Commission of the European Communities.

Neither the Commission of the European Communities, its contractors nor any person acting on their behalf:

make any warranty or representation, express or implied, with respect to the accuracy, completeness, or usefulness of the information contained in this document, or that the use of any information, apparatus, method or process disclosed in this document may not infringe privately owned rights; or

assume any liability with respect to the use of, or for damages resulting from the use of any information, apparatus, method or process disclosed in this document.

This report is on sale at the addresses listed on cover page 4

at the price of B.Fr. 70,—

**Commission of the
European Communities**
D.G. XIII - C.I.D.
29, rue Aldringen
L u x e m b o u r g
November 1972

This document was reproduced on the basis of the best available copy.

EUR 4880 e

RAPID DEPRESSURIZATION OF A THERMAL INSULATION SYSTEM FOR HIGH TEMPERATURE GAS REACTORS by E. ARANOVITCH and D. VAN ASSELT

Commission of the European Communities

Joint Nuclear Research Centre - Ispra Establishment (Italy)

Luxembourg, November 1972 - 54 Pages - 24 Figures - B.Fr. 70.—

This report presents the work carried out in collaboration with KFA Jülich, in order to study the behaviour of metall-foil multilayer thermal insulation bobbins under different depressurization rates. They should be able to withstand with helium under 25 atm. depressurization rates in the order of 20 atm/sec without damage.

The depressurization tests are completed with different control tests such as permeability tests, X-Ray photographs and metrology to evaluate modifications in the integrity of the bobbins.

A mathematical model and a correlation between permeability and depressurization tests are presented.

EUR 4880 e

COMMISSION OF THE EUROPEAN COMMUNITIES

RAPID DEPRESSURIZATION OF A THERMAL
INSULATION SYSTEM FOR HIGH TEMPERATURE
GAS REACTORS

by

E. ARANOVITCH and D. VAN ASSELT

1972



Joint Nuclear Research Centre
Ispra Establishment - Italy

ABSTRACT

This report presents the work carried out in collaboration with KFA Jülich, in order to study the behaviour of metall-foil multilayer thermal insulation bobbins under different depressurization rates. They should be able to withstand with helium under 25 atm. depressurization rates in the order of 20 atm/sec without damage.

The depressurization tests are completed with different control tests such as permeability tests, X-Ray photographs and metrology to evaluate modifications in the integrity of the bobbins.

A mathematical model and a correlation between permeability and depressurization tests are presented.

KEYWORDS

HTGR TYPE REACTORS	LEAKS
THERMAL INSULATION	MEASURED VALUES
FOILS	TESTING
METALS	NONDESTRUCTIVE TESTING
PRESSURE	MATHEMATICAL MODELS
TRANSIENTS	

<u>CONTENTS</u>	<u>Page</u>
1. Introduction	5
2. Description of Test Facility	6
3. Description of Test Bobbins	7
3.1 General Description	7
3.2 Modification of Test Bobbins	8
4. Instrumentation	8
4.1 Pressure Measurements	8
4.2 Differential Pressures	9
4.3 Strain Measurements	10
4.4 Temperature Measurements	10
5. Depressurization of the Vessel	11
6. Depressurization of the Insulation System into the Vessel	13
7. Experimental Results	15
7.1 Initial Depressurization Rates	20
7.2 Maximum Pressure Differences	20
8. Control Tests	23
8.1 Permeability Tests (Gas Flow Resistance Tests)	23
8.2 X-ray Photographs	27
8.3 Metrology	28
8.4 Leaktests	28
9. Correlation between Permeability and Depressurization Tests	30
Conclusions	31
Appendix	34
Nomenclature	35
List of Tables and Figures	37

RAPID DEPRESSURIZATION OF A THERMAL INSULATION SYSTEM FOR HIGH TEMPERATURE GAS REACTORS

by

E. Aranovitch and D. van Asselt

Contract of Collaboration: No. 014 - 70 - PISGD GHH/KFA, Jülich

1. INTRODUCTION

Insulation systems for high temperature gas reactors must not only show good characteristics from a thermal point of view, but must also fulfill other conditions, such as good behaviour under thermal cycling, pressure cycling, eventual corrosion phenomena, vibrations. They must be easy to mount and fix and be highly reliable, generally for the life time of the reactor.

The multilayer foil type of insulation is designed such as to keep the natural convection in the laminar range and in such systems, thermally speaking, it is better to have the individual cells as leaktight as possible in order to avoid macroconvection, that is fluid flow patterns covering the whole insulation system. But from a safety point of view, the insulation must be able to withstand accidental rapid depressurizations, due for instance to pump failure. In the case of a direct cycle, the initial depressurization rate could reach the order of 20 atm/sec in the primary ducts. Therefore there must be communications between the cells with the outside. A compromise must be found between these two contradictory aspects, safety and thermal performances.

The object of the present contract is to study the behaviour of DARCHEM type insulation bobbins under different depressurization rates. They should be able to withstand with helium under 25 atm depressurization rates in the order of 20 atm/sec without damage.

The depressurization tests are completed with different control tests such as permeability tests, radiography and metrology to evaluate modifications in the integrity of the bobbins.

The tests were carried out at the CCR Ispra on a test facility in which the depressurization rates can be made to vary up to more than 100 atm/sec.

The test program which was divided into two parts, started in April 1970, through to December 1970. The second part of the program was performed in the period January-October 1971. Two technical reports were written in the meantime, giving partial results. The present report represents the definitive report.

2. DESCRIPTIONS OF THE TEST FACILITY

A schematic design and a photograph of the depressurization facility are shown in Fig. 1 and 2. It mainly consists of a pressure vessel, internal diameter 610 mm, height 2450 mm, internal diameter of lid 570 mm. Working pressure 25 atm is in cold condition.

This facility offers the possibility to test either panels or bobbins up to 560 mm diameter and 1500 mm length, at an initial pressure up to 25 atm.

Different depressurization rates are obtained by variation of the diameter of a diaphragm through which the gas is escaping into the ambiance in the upper head of the vessel. The outlet diameter can be varied in mounting diaphragms of different diameters up to a maximum outlet of 200 mm, allowing depressurization rates between 0 and 200 atm/sec.

A double bursting disk system is fitted above the diaphragm (see Fig. 1). This system is built up as follows:

1. Flange welded on upper lid of vessel with metal ring joint
2. Diaphragm
3. Flange with mounting possibilities for diaphragm at lower side and burst-

ing disk at upper side

4. Lower bursting disk. Copper membrane, thickness 0.5 mm
5. Intermediate flange between lower- and upper bursting disk with gas inlet to pressurize space between bursting disks
6. Upper bursting disk copper membrane, thickness 2 mm
7. Endflange.

All flanges having 200 mm diameter openings.

Any non-corrosive gas can be used in the test rig. The tests are done with nitrogen or helium at room temperature with an initial pressure of 25 kg/cm^2 .

During pressurization of the vessel, the pressure between the two bursting disks is maintained at the same value as the vessel pressure. To burst the disks and thus open the outlet, the pressure in the space is suddenly raised to a value between 40 and 60 atm. That makes the upper disk burst followed immediately by the lower disk.

For measuring purposes, some studs are mounted on the vessel.

Furthermore, three holes are made in the vessel wall to make a leak-tight cable outlet for the instrumentation of the test piece (see Fig. 3).

3. DESCRIPTION OF THE TEST BOBBINS

3.1 General Description

The insulation to be tested (Fig. 4) was designed and fabricated by the DARCHEM Engineering Ltd., and is a cylindrical insulation for the primary ducts. In a mild steel tube two different insulation bobbins (length 605 mm, internal diameter 480 mm, outer diameter 540 mm) were mounted. Each bobbin is composed of 17 layers of stainless steel foil (thickness 0.1 mm), separated from each other by a wire mesh (square cells of 2", wire diameter 1.2 mm). The layers are enclosed between an inner- and an outer liner of stainless steel (thickness 1.6 mm). The only difference between the two

bobbins is in the design of the gas outlet.

Bobbin 4 is designed with two breather holes of 6 mm diameter opposite each other. Bobbin 3 is completely open at the end except ten 1" wide metal strips for mechanical stiffness. The ends of the bobbins are overlapping as to absorb thermal dilatation without increase of gas tightness.

The design is made in such a way that the geometry of these test bobbins is the same as the geometry of the real bobbin would be in the hot state under nominal temperature conditions.

3.2 Modifications of Test Bobbins

As will be seen in chapter 8.1, it was found that the greatest part of the gas flow resistance was concentrated on the overlapping of bobbin 3 and in the breather holes of bobbin 4. In order to reduce this resistance, 4 holes of diameter 6 mm were made in the overlapping of bobbin 3 (holes at 90° of each other, at 20 mm distance from the end of the overlap) (test series "B").

After these tests, in order to achieve in bobbin "3" a Δp of 1 kg/cm² at a depressurization rate with helium of 20 atm/sec, another modification was made. The 6 mm holes were closed and replaced by 4 holes of diameters 7.4, 6.4, 6 and 7.2 mm respectively, made close together in the overlaps of bobbins "3" and "4" (test series "C").

A last modification was carried out after test "C5". Ten holes of 7.2 mm diameter each were added to the 4 holes already present in the overlap of bobbin "4" and 14 additional holes of 7.2 mm diameter were drilled at 180° in the same overlap. Because of these 28 holes, all the gas flow resistance of bobbin "4" is concentrated in the breather holes and not in the overlap. (See table 7 , test series "D").

4. INSTRUMENTATION

4.1 Pressure Measurements

Absolute Pressures. To measure in the test rig the pressure drop as a

function of time, three absolute pressure transducers are mounted in the vessel. (For mounting position see Fig. 1). These transducers which were developed in our laboratories use a half bridge strain gauge circuit with a response time inferior to 30 microseconds (Fig. 5). The transducers are connected to a carrier frequency amplifier (BRANDAU multichannel amplifier, carrier frequency 6 kHz, bridge supply voltage 3 - 7.5 V) the output of which is connected to an U. V. -galvanometer recorder (S. E. L. ultra-violet light recorder, type SE 3012 50 channels, paper speed up to 3 m/sec, timing lines each 0.01 sec; galvanometers, type A 1000, natural frequency 1000 c/sec, flat frequency response 600 C/sec.).

4.2 Differential Pressures

Pressure differences are measured:

- a) between the inside of the test bobbin and the pressure vessel
- b) between the inside of pressure vessel and the circumferential gap by two different types of transducers.

For mounting position see Fig. 6.

The technical difficulties to overcome concerned mainly mounting space, 10 mm for the (b) type transducer, and the temperature effect during the expansion of the gas.

The basic parts of the (a) type transducers are:

- stainless steel membrane
- full bridge strain gauge circuit of 4 strain gauges IMP 220 - precision 2 x 2 mm
- pertinax housing

(See Fig. 7).

The membrane with strain gauges is mounted in between the two pertinax parts of the housing. The lower part can be screwed on the studs welded on the inner liner of the bobbins (Fig. 8).

relationship between temperatures at points A and D:

$$T_A = \frac{1+\chi}{2} \cdot T_D \quad (6)$$

We have thus a system of 7 equations with 7 unknowns, $P_A, P_D, \rho_A, \rho_D, T_A, T_D, U_D$ which are time dependent. By solving this system of equations it is found:

$$\frac{P_A}{P_{AO}} = \left[F(t) \right]^{\frac{2\chi}{\chi-1}} \quad (7)$$

$$\frac{P_D}{P_{AO}} = \left(\frac{2}{1+\chi} \right)^{\frac{\chi}{\chi-1}} \cdot \left[F(t) \right]^{\frac{2\chi}{\chi-1}} \quad (8)$$

$$\frac{\rho_A}{\rho_{AO}} = \left[F(t) \right]^{\frac{2}{\chi-1}} \quad (9)$$

$$\frac{\rho_D}{\rho_{AO}} = \left(\frac{2}{1+\chi} \right)^{\frac{\chi}{\chi-1}} \cdot \left[F(t) \right]^{\frac{2}{\chi-1}} \quad (10)$$

$$\frac{T_A}{T_{AO}} = \left[F(t) \right]^2 \quad (11)$$

$$\frac{T_D}{T_{AO}} = \frac{2}{1+\chi} \cdot \left[F(t) \right]^2 \quad (12)$$

$$\frac{U_D}{U_{DO}} = \left[F(t) \right] \quad (13)$$

where

$$F(t) = \frac{1}{1+at} \quad (14)$$

$$a = \frac{\chi-1}{2} \cdot \left(\frac{2}{1+\chi} \right)^{\frac{1}{\chi-1}} \cdot \left(\frac{2\chi}{1+\chi} \right)^{\frac{1}{2}} \cdot \frac{s_D}{V} \cdot \left(\frac{R}{M} \cdot T_{AO} \right)^{\frac{1}{2}} \quad (15)$$

These equations are valid as long as the pressure P_D at the diaphragm is greater than the external pressure P_e , or

$$P_A > \left(\frac{1+\kappa}{2}\right)^{\frac{\kappa}{\kappa-1}} \cdot P_e \quad (16)$$

In the case of air, for instance, $\kappa = 1.4$ and P_A should be 1.89 greater than P_e . In all tests the initial pressure is 25 kg/cm^2 and this set of equations is valid till the pressure in the vessel reaches 1.89 kg/cm^2 , that is the whole significant time for purposes of interest here. After that, St. Venant equations should be used. In the value of the cross-section s_D , a contraction coefficient of the order of 0.9 should be incorporated.

The value of the initial depressurization rate is:

$$\left(\frac{dP_A}{dt}\right)_{t=0} = - P_{AO} \cdot \frac{2\kappa}{\kappa-1} \cdot a \quad (17)$$

where "a" is given by equation (15).

Because the molecular weights and the values of " κ " are different with nitrogen and helium, the initial depressurization rate will be about 3 times greater with helium than with nitrogen under identical initial temperature and pressure conditions.

$$\left(\frac{dP_A}{dt}\right)_{t=0}^{\text{He}} = 3.12 \left(\frac{dP_A}{dt}\right)_{t=0}^{\text{N}_2} \quad \text{with} \quad \begin{aligned} \kappa_{\text{He}} &= 1.66 \\ \kappa_{\text{N}_2} &= 1.47 \end{aligned} \quad (18)$$

6. DEPRESSURIZATION OF THE INSULATION SYSTEM INTO THE VESSEL

As the vessel depressurizes, the pressure P_i in the insulation, follows the pressure P_A in the vessel with a certain delay. Experience shows that this delay, in the tests which were performed, is never great enough to get a sonic velocity at the outlets of the insulation bobbins and the set of equations used precedently is not valid here. From the point of view of the me-

chanical resistance of the insulation, the crucial point is reached when the difference $(P_i - P_A)$ is maximum. It is important to know the value of this maximum and the critical time t_{cr} at which it occurs. In order to evaluate these parameters, the assumption is made that the volume flow going out of the insulation into the vessel, can be written in the form:

$$\Delta P = P_i - P_A = \rho_i \cdot A \cdot Q_V^2 \quad (19)$$

where A is a form coefficient of dimensions $[L]^{-4}$, which can be a function of space in the insulation. In the paragraph concerning the permeability tests we shall elaborate more about the meaning and the restrictions implied in such a formula.

The volume flow Q_V is:

$$\rho_i Q_V = - \frac{d\rho_i}{dt} \cdot V_B \quad (20)$$

$$\text{with } \left(\frac{P_i}{P_{AO}} \right)^{1/\kappa} = \left(\frac{\rho_i}{\rho_{AO}} \right) \quad (21)$$

We have here a system of three equations with 3 unknowns, ρ_i , P_i , Q_V which, by combinations of equations (19), (20) and (21) leads to the following differential equation; written in a reduced system:

$$P_A^* = \frac{P_A}{P_{AO}}, \quad P_i^* = \frac{P_i}{P_{AO}}, \quad t^* = at \quad (22)$$

$$m^* \frac{dP_i^*}{dt} = - (P_i^* - P_A^*)^{1/2} \cdot (P_i^*)^{(1 - \frac{1}{2\kappa})} \quad (23)$$

$$\text{where } m^* = \frac{V_B}{V} \cdot s_D \cdot (A)^{1/2} \cdot g(\kappa) \quad (24)$$

$$g(\kappa) = \left(\frac{\kappa-1}{2\kappa} \right) \cdot \left(\frac{2}{1+\kappa} \right)^{\frac{1}{\kappa-1}} \left(\frac{2\kappa}{1+\kappa} \right)^{1/2} \quad (25)$$

When the function P_A^* is known, this differential equation (23) can be solved numerically. Using for P_A^* equation (7) numerical solutions were obtained

for different values of the dimensionless parameters m^* and χ .

It is interesting to see that this equation is independent of the molecular weight of the gas M and of the initial temperature T_{AO} . The nature of the gas is felt only through the value of χ .

The numerical solutions give two interesting characteristics of the depressurization phenomenon:

- the maximum value of the difference $(P_i^* - P_A^*)$
- the critical value t_{cr}^* at which this difference occurs.

Results are presented in tables 1 and 2.

The solutions of equation (23) can be used in different manners.

- (1) Once we know, either from permeability tests or from the first depressurization tests, the value of m^* for a given bobbin, the maximum value of $P_i^* - P_A^*$ can be known for any other depressurization conditions;
- (2) In a series of depressurization tests we can follow the value of A , which is connected to the integrity of the bobbin. Should the value of A start to vary in an effective manner, it would mean that the bobbin has been altered.

7. EXPERIMENTAL RESULTS

26 Depressurization tests were performed, 22 with nitrogen and 4 with helium. The tests have been divided in 4 different series depending on the different modifications of the bobbins "3" and "4". In every test the decrease of pressure in the vessel and the bobbins was recorded on recording paper, (see example in Fig. 9), giving the values of the following parameters:

- the initial depressurization rate $\left(\frac{dP_A}{dt}\right)_{t=0}$ in the vessel;
- the maximum value $(\Delta P)_{max}$ of the difference $P_i - P_A$ between the pressure in the bobbins and in the vessel;
- the maximum pressure difference $(\Delta P_g)_{max}$ between the circumferential

NUMERICAL SOLUTIONS OF EQUATION (23)

κ	m^*	at_{cr}	$\left(\frac{P_i - P_A}{P_{AO}}\right)_{max}$	κ	m^*	at_{cr}	$\left(\frac{P_i - P_A}{P_{AO}}\right)_{max}$
1.1	0.01	0.010	0.0372	1.3	0.01	0.007	0.0070
1.1	0.02	0.021	0.1035	1.3	0.02	0.018	0.0248
1.1	0.03	0.030	0.1671	1.3	0.03	0.031	0.0483
1.1	0.04	0.037	0.2223	1.3	0.04	0.042	0.0742
1.1	0.05	0.043	0.2696	1.3	0.05	0.053	0.1004
1.1	0.06	0.048	0.3102	1.3	0.06	0.063	0.1259
1.1	0.07	0.053	0.3456	1.3	0.07	0.071	0.1502
1.1	0.08	0.057	0.3766	1.3	0.08	0.080	0.1733
1.1	0.09	0.060	0.4040	1.3	0.09	0.087	0.1950
1.1	0.10	0.063	0.4286	1.3	0.10	0.094	0.2154
1.2	0.01	0.008	0.0129	1.4	0.01	0.006	0.0047
1.2	0.02	0.020	0.0427	1.4	0.02	0.017	0.0170
1.2	0.03	0.032	0.0785	1.4	0.03	0.029	0.0342
1.2	0.04	0.042	0.1148	1.4	0.04	0.041	0.0540
1.2	0.05	0.051	0.1494	1.4	0.05	0.053	0.0749
1.2	0.06	0.059	0.1814	1.4	0.06	0.064	0.0960
1.2	0.07	0.066	0.2109	1.4	0.07	0.074	0.1166
1.2	0.08	0.073	0.2379	1.4	0.08	0.083	0.1366
1.2	0.09	0.078	0.2628	1.4	0.09	0.091	0.1557
1.2	0.10	0.083	0.2856	1.4	0.10	0.099	0.1740

Table 1

NUMERICAL SOLUTIONS OF EQUATION (23) (contd.)

κ	m^*	at_{cr}	$\left(\frac{P_i - P_A}{P_{AO \max}}\right)$	κ	m^*	at_{cr}	$\left(\frac{P_i - P_A}{P_{AO \max}}\right)$
1.5	0.01	0.006	0.0035	1.7	0.01	0.005	0.0023
1.5	0.02	0.016	0.0129	1.7	0.02	0.014	0.0087
1.5	0.03	0.028	0.0264	1.7	0.03	0.026	0.0182
1.5	0.04	0.040	0.0424	1.7	0.04	0.035	0.0299
1.5	0.05	0.052	0.0598	1.7	0.05	0.050	0.0431
1.5	0.06	0.064	0.0777	1.7	0.06	0.062	0.0570
1.5	0.07	0.074	0.0956	1.7	0.07	0.074	0.0714
1.5	0.08	0.084	0.1132	1.7	0.08	0.085	0.0858
1.5	0.09	0.094	0.1304	1.7	0.09	0.095	0.1001
1.5	0.10	0.102	0.1469	1.7	0.10	0.105	0.1142
1.6	0.01	0.005	0.0028	1.8	0.01	0.005	0.0020
1.6	0.02	0.015	0.0103	1.8	0.02	0.014	0.0075
1.6	0.03	0.027	0.0215	1.8	0.03	0.025	0.0159
1.6	0.04	0.039	0.0350	1.8	0.04	0.037	0.0263
1.6	0.05	0.051	0.0499	1.8	0.05	0.050	0.0381
1.6	0.06	0.063	0.0656	1.8	0.06	0.062	0.0507
1.6	0.07	0.074	0.0815	1.8	0.07	0.073	0.0639
1.6	0.08	0.085	0.0973	1.8	0.08	0.085	0.0772
1.6	0.09	0.095	0.1129	1.8	0.09	0.095	0.0905
1.6	0.10	0.104	0.1280	1.8	0.10	0.106	0.1036

Table 2

gap and the outside of the bobbins - Fig. 4;

- the critical times t_{cr} and t_{gcr} at which these maxima occur;
- the approximate maximum temperature drop ΔT of the gas in the pressure vessel.

The experimental results are presented in tables 3 and 4.

EXPERIMENTAL RESULTS

Test No.	Gas	Diaph. ϕ mm	$\left(\frac{dP_A}{dt}\right)_{t=0}$	BOBBIN "3"		BOBBIN "4"	
				$(\Delta P)_{max}$ kg/cm ²	t_{cr} sec	$(\Delta P)_{max}$ kg/cm ²	t_{cr} sec
A-1	N ₂	5.6	0.54	0.022	0.9	0.011	0.9
A-2	N ₂	12.5	1.23	0.157	0.9	0.100	0.9
A-3	N ₂	13.7	1.65	0.202	1.3	0.130	1.0
A-4	N ₂	15	1.85	0.247	1.1	0.174	1.0
A-5	N ₂	16.5	2.00	0.261	1.1	0.188	0.9
A-6	N ₂	18.3	2.38	0.452	1.3	0.330	1.0
A-7	N ₂	19.1	2.73	0.472	1.3	0.379	1.1
A-8	N ₂	20.1	3.17	0.532	1.2	0.430	0.9
A-9	N ₂	21.1	3.30	0.604	1.3	0.511	1.2
A-10	N ₂	22.5	3.70	0.728	1.3	0.637	1.1
A-11	N ₂	23.6	3.85	0.865	1.3	0.805	1.3
A-12	He	19.1	7.80	0.940	0.6	1.100	0.7

Table 3

In the series of tests "A", the values of $(\Delta P)_{gmax}$ and t_{gcr} were not recorded. From the recorded curves, it was difficult to determine with a great precision the exact values of the critical times; so, for the test series "B", "C" and "D" intervals are given.

EXPERIMENTAL RESULTS

Test No.	Gas	T °C	Diaph. Ø mm	$\left(\frac{dP}{dt}\right)_{t=0}$ atm/sec	BOBBIN "3"				BOBBIN "4"			
					$(\Delta P)_{max}$ kg/cm ²	t _{cr} sec	$(\Delta P_g)_{max}$ kg/cm ²	t _{g cr} sec	$(\Delta P)_{max}$ kg/cm ²	t _{cr} sec	$(\Delta P_g)_{max}$ kg/cm ²	t _{g cr} sec
B-1	N ₂	35	11	1.0	0.015	0.90	0.025	0.1	0.065	0.9	0.015	0.1
B-2	N ₂	50	16.5	2.0	0.075	0.60-0.90	0.075	0.5	0.225	0.90-1.45	0.040	0.5
B-3	N ₂	53	19.5	2.3	0.160	0.50-0.70	0.140	0.5	0.395	0.90-1.10	0.075	0.5
B-4	N ₂	67	24.2	4.4	0.305	0.65-0.75	0.375	0.65-0.75	1.165	1.55-1.65	0.160	1.55
B-5	N ₂	-	26.2	5.0	0.370	0.60-0.80	0.380	0.60-0.80	1.365	1.50-1.80	0.170	1.50
C-1	N ₂	50	16.5	2.4	0.090	0.70-0.90	0.095	0.50-0.80	0.205	0.90-1.10	0.030	0.30-1.00
C-2	He	65	18.0	7.0	0.235	0.18-0.24	0.245	0.18-0.24	0.590	0.37-0.54	0.095	0.37-0.54
C-3	N ₂	64	24.0	4.4	0.325	0.65-0.75	0.320	0.65-0.75	0.800	1.15-1.25	0.095	1.15-1.25
C-4	N ₂	67	26.2	5.0	0.410	0.61-0.71	0.445	0.55-0.75	1.350	1.50-1.85	0.130	1.60
C-5*	He	80	26.2	16.1	0.850	0.23	0.885	0.23	1.630*	0.23	0.115	0.23
D-1	N ₂	70	29.0	7.2	0.425	0.50-0.68	0.410	0.50-0.68	0.640	0.90-1.10	0.050	0.90-1.10
D-2	N ₂	74	31.5	8.3	0.570	0.57-0.67	0.575	0.52-0.62	1.210	1.35-1.65	0.060	-
D-3	N ₂	74	34.0	8.5	0.730	0.57-0.66	0.700	0.57-0.66	1.530	1.22-1.44	0.060	1.22-1.44
D-4*	He	74	30.0	19.2	0.860	0.20-0.26	0.845	0.23	1.800*	0.39	0.085	0.335

* - Buckling. For more information, see table 5.

Table 4

7.1 Initial Depressurization Rates $\left(\frac{dP_A}{dt}\right)_{t=0}$

In Fig. 10 the initial depressurization rate $\left(\frac{dP_A}{dt}\right)_{t=0}$ is plotted versus the diameter square of the diaphragm (proportional to the cross-section area of the diaphragm in which a contraction coefficient of 0.9 has been accounted for). As was said before, it can be noted that for the same diaphragm with the same initial static pressure, the depressurization rate is greater with helium than with nitrogen. In this Fig. 10 the experimental data is compared with the calculated curves. The agreement between theory and experience is quite satisfactory. The experimental values of $\left(\frac{dP_A}{dt}\right)_{t=0}$ are obtained by graphical methods from the recorded absolute pressure curves with a precision of the order of 5%.

7.2 Maximum Pressure Differences

Between the different series of tests "A", "B", "C" and "D" modifications were performed on the bobbins which are described in chapter 3.2.

In Fig. 11 and Fig. 12 the maximum pressure difference $(\Delta P)_{\max}$ is plotted versus the initial depressurization rate for each series of tests.

The first series of tests "A" showed that the two tested bobbins would not satisfy the initial requirement of a value of the $(\Delta P)_{\max}$ inferior to 1 kg/cm^2 with helium under an initial depressurization rate of 20 atm/sec. In these tests, with a depressurization rate of 7.8 atm/sec, $(\Delta P)_{\max}$ of 0.94 kg/cm^2 and 1.1 kg/cm^2 were recorded for bobbins "3" and "4".

In tests series "B" it can be noted that the modifications performed after the "A" tests were successful in reducing the values of $(\Delta P)_{\max}$ in bobbin "3". Bobbin "4" had not been altered. It can be noted that for bobbin "3" the values of $(\Delta P)_{\max}$ and $(\Delta P)_g_{\max}$ are about the same, because the grid system introduces little additional resistance. For bobbin "4" the values of $(\Delta P)_{\max}$ are much higher than the values of $(\Delta P)_g_{\max}$ because the breather holes introduce an important additional resistance.

The test series "C" show that modifications performed after the "B" tests had not changed results concerning bobbin "3" but had reduced slightly the values of $(\Delta P)_{\max}$ for bobbin "4", but not sufficiently to avoid a severe buckling damage in this bobbin, (with a depressurization rate of 16.1 atm/sec. the value of the $(\Delta P)_{\max}$ was 1.63 kg/cm², test No. C-5). The shape of the registered curve of this last test confirmed that the buckling had effectively taken place at this point; Fig. 13 and Fig. 14. In Fig. 13 it can be seen that at critical time t_{cr} the ΔP diminishes suddenly, because of the increase of volume after buckling. In Table 5 the values are presented of the different parameters involved in this phenomenon. At times t_{cr} and t_{gcr} the curves of strain gauge measurements showed a very steep peak due to an important increase of strain. The dimensions of the lump formed after buckling were: length about 58 cm, width about 22 cm, height about 2.5 cm (see metrology). The buckling happened along the axial weld of the inner liner.

Between tests "C" and "D", bobbin "3" was not modified. The changes in the experimental results for this bobbin were due to the influence of the buckling of bobbin "4". For bobbin "4" the changes in the experimental results when passing from tests "C" to tests "D" are due partly to buckling and partly to the modifications performed on this bobbin after the "C" tests. In test D-4 the bobbin "4" suffered buckling damage again, of the same type as in test C-5. After dismounting, two other lumps were noted in bobbin "4" (dimensions 60x27 cm).

In Fig. 15 a comparison is made between experimental results, presented in a reduced system, and theoretical curves obtained from the mathematical model presented in Chapter 6. It can be noted that the experimental values of $(\Delta P)_{\max}$ are slightly inferior to the calculated values of $(\Delta P)_{\max}$. (One should not forget the experimental imprecision in the determination of $\left(\frac{dP}{dt}\right)_{t=0}$ and t_{cr} , and the approximations in the mathematical model).

RESULTS OF TESTS C-5 AND D-4

Test	Bobbin	$(\Delta P)_{\max}$	t_{cr}	ΔP_1°	Δt	$(\Delta P)_{\max 2}$	$t_{cr 2}$	$(\Delta P_g)_{\max}$	$t_{g cr}$	ΔP_g°	Δt_g	$(\Delta P_g)_{\max 2}$	$t_{g cr 2}$
C-5	3	0.850	0.23	0.820	≈ 0.006	< 0.820	-	0.885	0.23	0.825	≈ 0.006	< 0.825	-
	4	1.630	0.23	1.150	0.006	1.500	0.72	0.115	0.23	0.023	≈ 0.006	0.197	0.80
D-4	3	0.860	0.225	-	-	-	-	0.845	0.225	-	-	-	-
	4	1.800	0.385	1.120	0.01	1.550	0.85	0.085	0.385	0.025	0.01	0.095	1.05

Table 5

8. CONTROL TESTS

In order to evaluate eventual damage to the structural integrity of the bobbins, 4 kinds of tests are performed:

- permeability tests,
- X-ray tests,
- metrology,
- leaktightness of welds.

8.1 Permeability Tests (Gasflow Resistance Tests)

Permeability tests performed before and after depressurization tests give important indications of alteration in the integrity of the bobbins and can be used to evaluate the $(\Delta P)_{\max}$ at different depressurization rates. We define here the permeability in a rather large sense as the resistance to a fluid flow between two points in the bobbin. In steady state conditions, the ΔP against volume flow can be written in the following form:

$$\frac{\Delta P}{Q_v^2} = \rho A_1 + \mu \frac{B_1}{Q_v}$$

The first term accounts for pressure drop due to the loss of dynamic pressure and turbulent flow. The second term accounts for laminar friction.

A_1 has the dimension $[L^{-4}]$;

B_1 has the dimension $[L^{-3}]$.

If we plot $\Delta P/Q_v^2$ versus $1/Q_v$ we should obtain a straight line from which A_1 and B_1 could easily be deduced.

So if after a series of depressurization tests, the bobbin has suffered internally, one can expect modifications in the values of the coefficients A_1 and B_1 .

Tests were carried out at ambient temperature with nitrogen. The pressure drop was measured by an inclined water manometer and the volume flow was measured by a rotameter flowmeter. For the in- and outlet of the

gas, eight bolts were welded on the inner liner. For test set-up see Fig. 16; for permeability connections see Fig. 17; for mounting position see Fig. 6

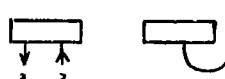
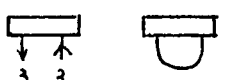
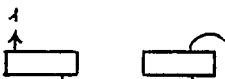
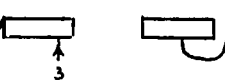
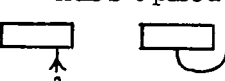
When the measurement is made on one bobbin, all the openings in the other one (such as overlapping, modification holes, permeability connections and transducer holes) are closed.

Five different types of permeability measurements are made with nitrogen before and after each modification or tests series:

- 1) The gas is injected through three connections at the front of the bobbin. (A; see Fig. 17) and leaves the bobbin through three connections at the end (B; see Fig. 17). The pressure drop is measured between the fourth front connection and the atmosphere. All other openings are closed. See tables 6 and 7, Scheme 1).
- 2) Same as for 1). Pressure drop is measured between fourth front and fourth end connections (see Scheme 2).
- 3) Gas injection through 3 front connections. Gas outlet through hole in mild steel tube (C; see Fig. 17). Pressure drop is measured between fourth front connection and other hole in mild steel tube. All other openings are closed (see Scheme 3).
- 4) Gas injection through 3 front connections. Gas outlet through overlap (D; see Fig. 17). Pressure drop is measured between fourth front connection and atmosphere. Modification holes and all other openings are closed (see Scheme 4).
- 5) Same as for 4). Modification holes in overlap are opened (see Scheme 5).

The results are shown in tables 6 and 7 and represented in Fig. 17 and Fig. 18.

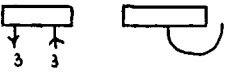
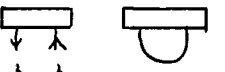
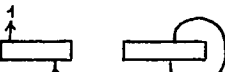
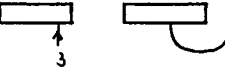
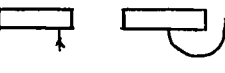
RESULTS OF PERMEABILITY TEST BOBBIN "3"

Test No.	Chronology	ΔP for Q_v m ³ /h			Measuring points	Observations
		5	10	15		
1a	before A series		23	63		4 holes 90°
1b	after A series		32	73		
1c	before B series		27	62		
1d	after B series		31	72		
1e	before C series		26	69		
1f	after C series		31	81		
1g	after D series		39	76		
2a	before A series		0	0		internal resistance negligible small effect is observed 4 holes 90° 4 holes A small effect is observed
2b	after A series		2	4		
2c	before B series		2	3		
2d	after B series		2	4		
2e	before C series		2	4		
2f	after C series		3	6		
2g	after D series		2	3		
3a	before A series		0	0.4		the grid has no effect 4 holes 90° 4 holes
3b	after A series		3	5		
3c	before B series		2	4		
3d	after B series		-	-		
3e	before C series		-	-		
3f	after C series		-	-		
3g	after D series		4.5	7.5		
4a	before A series	186	522		modification holes closed 	all resistance concentrated in the overlap 4 holes 90° 4 holes. Deformation of inner liner Bobbin "4" or deformation of overlap (v. 5 e/f). Stronger deformation
4b	after A series	174	520	1031		
4c	before B series	174	520	1031		
4d	after B series	170	506	992		
4e	before C series	143	392	816		
4f	after C series	125	221	433		
4g	after D series	63	184	357		
5c	before B series	30	106	220	modification holes opened 	4 holes 90° 4 holes. Deformation of inner liner Bobbin "4" or deformation of overlap (v. 4 e/f)
5d	after B series	34	111	230		
5e	before C series	33	113	236		
5f	after C series	25	80	160		
5g	after D series	25	74	150		

ΔP is expressed in mm H₂O

Table 6

RESULTS OF PERMEABILITY TESTS BOBBIN "4"

Test No.	Chronology	ΔP for Q_v m ³ /h			Measuring points	Observations
		5	10	15		
1a 1b 1c 1d 1e 1f 1f ₁ 1g	before A series after B series before B series after B series before C series after C series before D series after D series		35 42 37 48 43 39 44 53	94 89 84 105 97 78 79 117		4 holes. Deformation caused by buckling 28 holes. Deformation caused by buckling
2a 2b 2c 2d 2e 2f 2f ₁ 2g	before A series after A series before B series after B series before C series after C series before D series after D series		1 4 6 7 7 5 3 3	10 8 10 13 13 10 5 5		there is a small internal resistance 4 holes. Deformation caused by buckling 28 holes. Deformation caused by buckling
3a 3b 3c 3d 3e 3f 3f ₁ 3g	before A series after A series before B series after B series before C series after C series before D series after D series	44 79 82 64 - - 41 54	218 285 293 295 - - 116 188			the hole design gives a much greater resistance than the grid 4 holes 28 holes
4a 4b 4c 4d 4e 4f 4f ₁ 4g	before A series after A series before B series after B series before C series after C series before D series after D series	103 109 113 116 110 65 65 85	343 380 395 394 398 210 205 277	851 884 865 870 427 403 579		important resistance in overlap 4 holes 28 holes. Deformation of overlap modification holes closed
5c 5d 5e 5f 5f ₁ 5g	before B series after B series before C series after C series before D series after D series	- - 97 53 38 60	- - 344 165 119 209	- - 753 360 251 457		4 holes 28 holes. Deformation of overlap

ΔP is expressed in mm H₂O

Table 7

Bobbin "3"

- for tests "1" the internal resistance plus the dynamic pressure are measured. The effect of the modifications between tests series "B", "C" and "D" is very small.
- for tests "2" only the internal resistance is measured. It is negligible.
- for tests "3" the grid resistance is measured; negligible.
- for tests "4" the resistance of the overlapping is measured with modification holes closed. All resistance is concentrated in the overlapping (A series). These tests showed for series "C" and "D" a sensible diminution in the resistance of the overlapping.
- for tests "5" the resistance of the overlapping is measured with open holes. Here also comparing values before and after tests series "C" and "D" it can be observed that the resistance of the overlapping has diminished.

Bobbin "4"

- for tests "1" internal pressure plus the dynamic pressure are measured. The effect of the modifications between tests series "B", "C" and "D" is very small. The effect of the buckling is significant.
- for tests "2" only internal resistance is measured. It is negligible.
- for tests "3" the resistance of the breather holes is measured. There is a measurable effect after buckling.
- for tests "4" resistance of the overlapping is measured with the modification holes closed. Here too an important resistance in the overlapping. For the "C" and "D" series a notable deformation of the overlapping is measured.
- for tests "5" resistance of the overlapping is measured with open holes; the same effect as for tests "4" is noted.

8.2 X-Ray Photographs

Displacement of the wire mesh at the interior of the bobbin that might occur due to gas flow velocity is controlled with X-ray photography.

Before and after depressurization tests X-ray photographs are made at three different reference points of the test tube. See Fig. 20.

Inspection of the picture shows no important axial and tangential displacement of the mesh wires. Example see Fig. 21.

8.3 Metrology

The internal diameters of test tube are measured before and after testing to investigate eventual changes due to depressurization; see Fig. 23. The results are given in table 8.

It can be noticed that:

- after depressurization test A-12 there are no changes;
- after depressurization test B-5 no important changes occur, except for measuring point 11;
- after depressurization test C-5 not only on bobbin "4" important deformations are measured but diameters of bobbin "3" are changed as well; especially the overlap (measuring points 7, 19, 31 and 43);
- after depressurization test D-4 there are important changes on bobbin "3".

8.4 Leaktests

In order to notice eventual damage of the welds between outer liner and mild steel tube, these welds of bobbins "3" and "4" are leak tested. Therefore a nitrogen pressure of resp. 10 and 20 g/cm² is put into the bobbin and the gas flow through the weld is measured. For test method, see Fig. 23. As can be seen from table 9, the weld of bobbin "4" changes during depressurization.

Test no. 1 before depressurization test A-1
 Test no. 2 after depressurization test A-12
 Test no. 3 before depressurization test B-1
 Test no. 4 after depressurization test B-5
 Test no. 5 after depressurization test C-5
 Test no. 6 after depressurization test D-4

METROLOGY

Measuring points	Diameter mm					
	test 1	test 2	test 3	test 4	test 5	test 6
1	480.40	480.42	480.42	480.48	480.65	480.82
2	478.75	478.74	478.74	478.75	479.09	479.48
3	478.58	478.50	478.50	478.60	478.82	479.16
4	477.52	477.45	477.45	477.38	477.30	476.84
5	477.35	477.28	477.28	477.35	476.63	475.39
6	479.13	479.13	479.13	479.12	477.73	475.92
7	480.40	480.21	480.21	480.30	477.84	475.64
8	479.88	479.70	479.90	479.72	475.09	472.63
9	478.32	478.22	478.22	478.21	463.07	450.40
10	476.64	476.56	476.57	476.65	458.71	431.00
11	477.72	477.56	477.56	476.67	463.96	451.10
12	477.85	477.72	477.72	477.76	476.57	475.30
13	476.57	476.68	476.68	476.65	476.97	476.29
14	473.64	473.73	473.73	473.70	473.38	472.96
15	472.26	472.24	472.24	472.23	472.05	471.46
16	476.17	476.23	476.23	476.25	476.31	476.67
17	477.78	477.83	477.83	477.82	478.27	479.46
18	477.90	477.90	477.90	477.92	478.67	481.10
19	475.46	475.50	475.50	475.23	476.43	480.75
20	474.76	474.83	474.83	474.77	475.95	482.5
21	480.03	480.04	480.04	480.04	481.00	485.6
22	480.82	480.84	480.84	480.80	481.43	485.0
23	480.46	480.49	480.49	480.47	481.16	485.1
24	478.56	478.55	478.55	478.45	479.18	479.8
25	481.28	481.29	481.29	481.38	481.30	481.46
26	481.80	481.79	481.79	481.82	482.00	482.45
27	481.75	481.80	481.80	481.89	481.95	482.32
28	484.50	481.58	481.58	481.60	481.50	481.88
29	480.60	480.71	480.71	480.72	480.35	478.40
30	479.90	480.04	480.04	480.00	479.46	475.47
31	477.39	477.59	477.59	477.44	476.55	469.5
32	477.08	477.16	477.16	477.15	476.25	464.7
33	479.50	479.63	479.63	479.63	479.13	445.5
34	480.10	480.27	480.27	480.24	480.07	441.3
35	480.76	480.94	480.94	480.91	480.95	450.7
36	479.68	479.83	479.83	479.80	480.07	479.1
37	483.70	483.54	483.54	483.59	483.67	483.46
38	483.41	483.15	483.15	483.21	483.16	482.76
39	483.29	483.18	483.18	483.27	483.00	482.85
40	485.00	484.92	484.92	484.97	485.18	485.80
41	485.08	485.00	485.00	485.02	485.65	487.2
42	484.42	484.38	484.38	484.41	485.52	488.2
43	482.53	482.54	482.54	482.46	484.14	488.2
44	482.54	482.49	482.49	482.48	484.79	489.6
45	484.37	484.34	484.34	484.34	487.13	493.2
46	483.41	483.44	483.44	483.37	486.66	494.8
47	482.24	482.26	482.26	482.23	484.31	490.0
48	478.92	478.92	478.92	478.89	479.07	480.49

table 8

LEAK TEST

Bobbin	Press. g/cm ²	Before depr.	Leak cc/min			
			after depressurization Test No.			
			A-12	B-5	C-5	D-4
3	10	0	0	0	0	0
	20	0	0	0	0	0
	40	0	-	-	-	0
4	10	1400	0	0	0	0
	20	2200	0	0	215	0
	40	-	-	-	-	0

table 9

9. CORRELATION BETWEEN PERMEABILITY AND DEPRESSURIZATION TESTS

In chapter 6 we have shown that the internal pressure P_i in the bobbin and the pressure P_A in the vessel can be related by the following differential equation

$$m^* \frac{dP_i^*}{dt^*} = - (P_i^* - P_A^*)^{1/2} \cdot P_i^{*(1 - \frac{1}{2\chi})}$$

where $m^* = \frac{V_B}{V} \cdot s_D \cdot (A)^{1/2} \cdot g(\chi)$

and $g(\chi) = \left(\frac{\chi-1}{2\chi}\right) \cdot \left(\frac{2}{1+\chi}\right)^{1/(\chi-1)} \cdot \left(\frac{2\chi}{1+\chi}\right)^{1/2}$

Numerical solutions of the differential equation give

- either the values of the maximum pressure difference $(\Delta P)_{\max}^*$ as a function of m^* and χ ,
- or the values of the critical time t_{cr}^* as a function of the same parameters m^* and χ . See tables 1 and 2.

Inversely, from experimental tests which gave the values of the maxi-

imum pressure difference $(\Delta P)_{\max}$ and the critical time t_{cr} , we can determine the values of m^* , that is of A , if V_B , V , s_D and χ are known. A_1 is also given by the permeability tests in the form of equation:

$$\frac{\Delta P}{Q_v^2} = \rho A_1 + \mu \frac{B_1}{Q_v} \quad \text{with } A_1 \neq A$$

So it is possible to compare the values of A_1 given either by the depressurization tests or the permeability tests.

From the results of the depressurization tests we determine m^* , and therefore A , either from the experimental values of the critical time t_{cr} or from the experimental values of $(\Delta P)_{\max}$ (using tables 1 and 2).

The results are represented in Fig.22 which gives a kind of chronological history of the whole series of tests.

As far as the bobbin "3" is concerned, it can be noticed that tests "B" did not modify the values of A_1 , but that after tests "C" the values of A_1 had diminished. As far as bobbin "4" is concerned, buckling appeared at the end of tests "C". For this reason tests "D" are not represented.

If we take into account the different simplifying assumptions which have been made, (for instance that the flow resistance is identical in steady conditions with permeability tests as in transient conditions with depressurization tests), it can be concluded that there exists a fairly good correlation between flow resistance in permeability tests and in depressurization tests.

CONCLUSIONS

We have exposed the results of a series of depressurization tests on two slightly different DARCHEM type insulation bobbins. 26 Depressurization tests were performed, 22 with nitrogen and 4 with helium. The tests have been divided into 4 different series depending on the different modifications performed on the bobbins. All tests were done in the cold state with an ini-

tial pressure of 25 kg/cm^2 . In one bobbin the modifications were successful in maintaining the value of $(\Delta P)_{\text{max}}$ (maximum pressure difference between inside and outside of the bobbin) inferior to 1 kg/cm^2 with a depressurization rate of the order of 20 atm/sec . For the other bobbin, in which the design of the overlapping was different, the modifications could not keep the values of $(\Delta P)_{\text{max}}$ inferior to 1 kg/cm^2 and this bobbin was severely damaged by buckling phenomena (with a depressurization rate of 16 atm/sec ; before the first buckling a ΔP of 1.63 kg/cm^2 was measured).

From an analysis of the permeability tests which were made on the two bobbins, it can be concluded that the flow resistance is not so much due to the internal structures of the bobbins, but rather to design details concerning the overlappings between two adjacent bobbins.

A mathematical model is presented from which it is possible to calculate the maximum ΔP in the bobbin as a function of the depressurization rate. Agreement between theoretical calculations and experimental results is fairly satisfactory. This model confirms that the laminar flow resistance in the internal structure of the insulation is negligible compared to the dynamic pressure resistance.

X-rays control tests showed little alteration in the wire mesh distributions before and after the tests.

From an instrumentation point of view, we had to overcome some initial difficulties concerning the pressure transducers which were too temperature sensitive. It was found that the plastic pressure transducers were not fully reliable (modification of calibration curves with time). All results presented here are based on data given by the stainless steel pressure transducers.

As a general conclusion it can be stated that the insulation bobbins as they were designed initially, would not meet the requirements of a ΔP of 1 kg/cm^2 with a depressurization rate of 20 atm/sec with helium under a

pressure of 25 kg/cm^2 . Little flow resistance is offered by the wire mesh or the "normal inside" of the bobbin. This resistance is all concentrated in the extremities (overlappings, breather holes). These are the points which should be modified. Modifications will be easier with the bobbins with the grid system, than with the bobbins with the breather holes. Tests show that the mechanical resistance of the bobbins is satisfactory up to values of the ΔP of the order of 1 kg/cm^2 .

ACKNOWLEDGEMENTS

We wish to thank Dr. BROCKERHOF and Dr. HEINECKE of KFA Jülich for their contribution in the planning, discussion and interpretation of results presented in this report. We also wish to thank Messrs. BENUZZI, DUFRESNE and FARFALETTI of C.C.R. Ispra for their help in the preparation of this work.

APPENDIX

Control Tests of Transducers

For the ΔP measurement between the inside of the bobbin and pressure vessel initially two different types of pressure transducers were foreseen, i. e. four with glass fiber reinforced epoxy resin membranes and two with stainless steel membranes. As resulted from the tests, the ΔP values given by the transducers with stainless steel membranes were always much higher than the values of the other two transducers. To explain this phenomena, some control tests were done with the transducers.

Static tests showed that the transducers with stainless steel membranes were very stable and showed the same test curves with intervals for over two months. The transducers with epoxy resin membranes were not stable and showed an important aging effect. Therefore in table 1 the results of $(\Delta P)_{\max}$ are the values measured by the middle transducer with stainless steel membrane.

Some dynamic tests are carried out to measure the response time and eventual overshoot of the transducer. For a schematic view of the test setup, see Fig. 23.

The pressure vessel, having a volume of about 10 l, is pressurized up to a known nitrogen pressure e. g. 2 atm. With the gas outlet closed, the solenoid valve is opened and the nitrogen flows into the test vessel. While the volume of the test vessel is 20 cm³ only, the pressure drop in the system is negligible.

After about 2 seconds the gas outlet is opened. The response time of the system is limited by the opening time of the solenoid valve, the gas flow velocity between pressure vessel and test vessel and the response time of the transducer.

Test results: response time < 20 msec; no measurable overshoot. See example on photograph 24.

NOMENCIATURE

a	time coefficient in depressurization formula
A, A ₁	form coefficients related to dynamic pressure
B ₁	form coefficient related to laminar flow resistance
C _P , C _V	specific heat at constant pressure and volume
g(κ)	function of κ
M	molecular weight
m*	dimensionless coefficient
P _A	pressure in depressurization vessel at time t
P _{AO}	initial pressure at time t = 0
P _D	pressure in diaphragm cross section
P _e	external pressure
P _i	pressure inside the bobbin
P _A [*] , P _i [*]	pressures in reduced system
Q _m	mass flow
Q _v	volume flow
R	constant of perfect gases
s _D	cross section area of diaphragm
t	time
t _{cr}	critical value of t for which ΔP is maximum
t _{cr} [*]	critical value of t in a reduced system
T _A	absolute temperature in vessel
T _{AO}	absolute temperature at time t = 0
T _D	absolute temperature in diaphragm
U _D	sonic velocity in diaphragm
U _{DO}	sonic velocity at time t = 0
V	gas volume in vessel
V _B	gas volume in bobbin
ρ _A	density of gas in vessel
ρ _{AO}	density of gas at time t = 0
ρ _D	density of gas at diaphragm
ρ _i	density of gas inside the bobbin
κ	κ = C _P /C _V

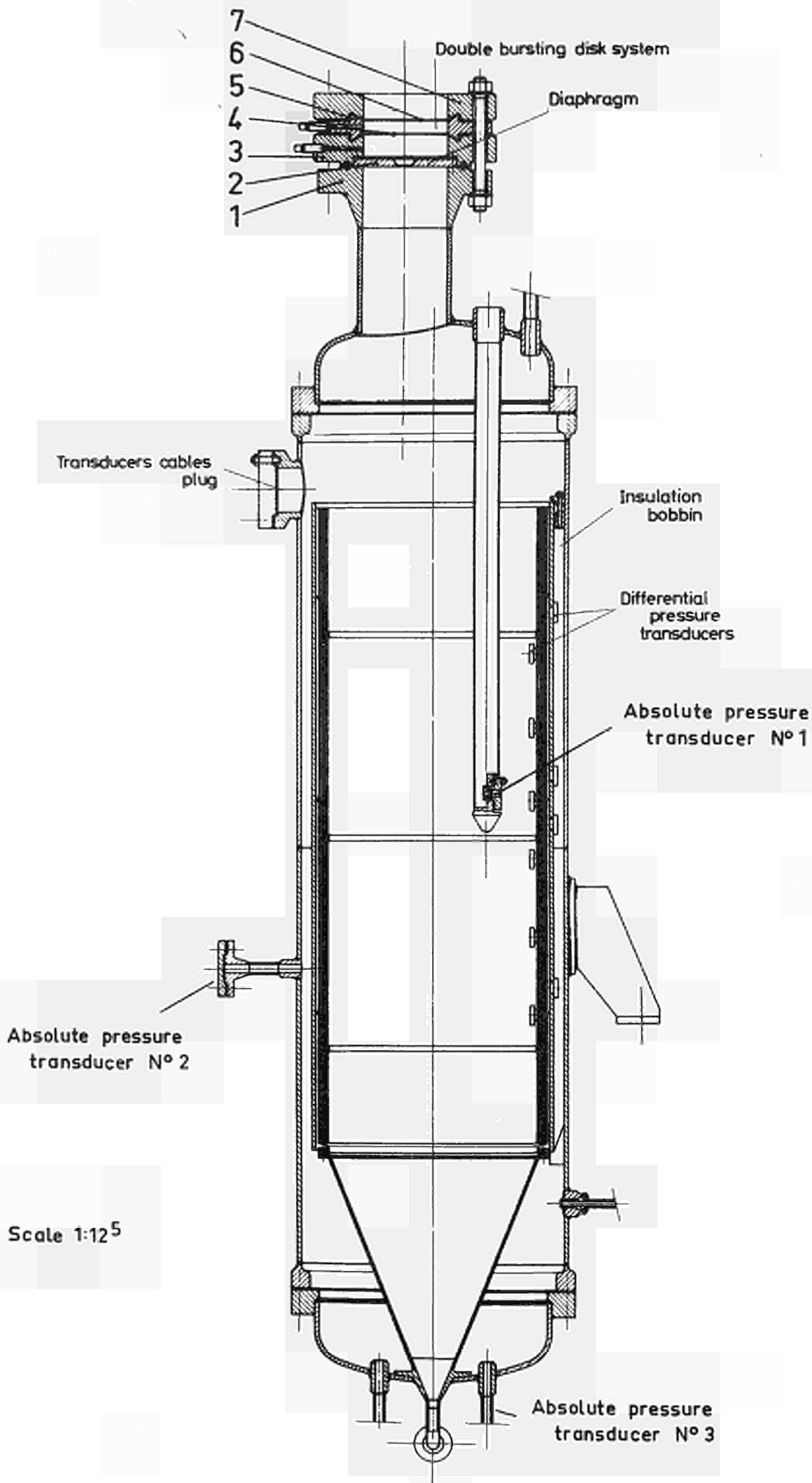
μ	dynamic viscosity of gas
ΔP	$= P_i - P_A =$ pressure difference between inside and outside of the bobbin
$(\Delta P)_{\max}$	maximum value of ΔP
$(\Delta P)_{\max}^{\#}$	maximum value of ΔP in a reduced system
$t_{g\ cr}$	critical value of t for which ΔP_g is maximum
t_{cr2}	critical time after buckling; see Fig. 13
$t_{g\ cr2}$	critical time t_g after buckling; see Fig. 13
ΔP_g	difference of pressure between inside and outside of the mild steel tube
$(\Delta P)_{\max2}$	maximum value of ΔP after buckling; see Fig. 13
$(\Delta P)_{g\ \max}$	maximum value of ΔP_g
$(\Delta P)_{g\ \max2}$	maximum value of ΔP_g after buckling; see Fig. 13
Δt	time during which ΔP drops during buckling
Δt_g	time during which ΔP_g drops during buckling
ΔT	temperature drop of gas in vessel

LIST OF TABLES AND FIGURES

- Fig. 1 - Schematic design of test facility
- " 2 - Photograph of test facility
- " 3 - Leaktight cable outlet
- " 4 - Schema of insulation bobbin
- " 5 - Cross-section of pressure transducer (absolute)
- " 6 - Mounting points for ΔP and permeability measurements
- " 7 - Differential pressure transducer (a-type)
- " 8 - Differential pressure transducers
- " 9 - Example of enregistered curves
- " 10 - Depressurization rate versus diaphragm diameter square
- " 11 - Experimental results bobbin "3"
- " 12 - " " " " "4"
- " 13 - Example of enregistered curves during buckling
- " 14 - Photograph of bobbin after buckling
- " 15 - Comparison between experimental and theoretical results
- " 16 - Test set-up for permeability measurement
- " 17 - Permeability connections
- " 18 - Results of permeability tests bobbin "3"
- " 19 - " " " " "4"
- " 20 - Measuring points metrology and position of X-ray photographs
- " 21 - X-Ray photographs
- " 22 - Correlation between permeability and depressurization tests
- " 23 - Test set-up for differential pressure transducers (schematic)
- " 24 - Photographs of dynamic pressure recording

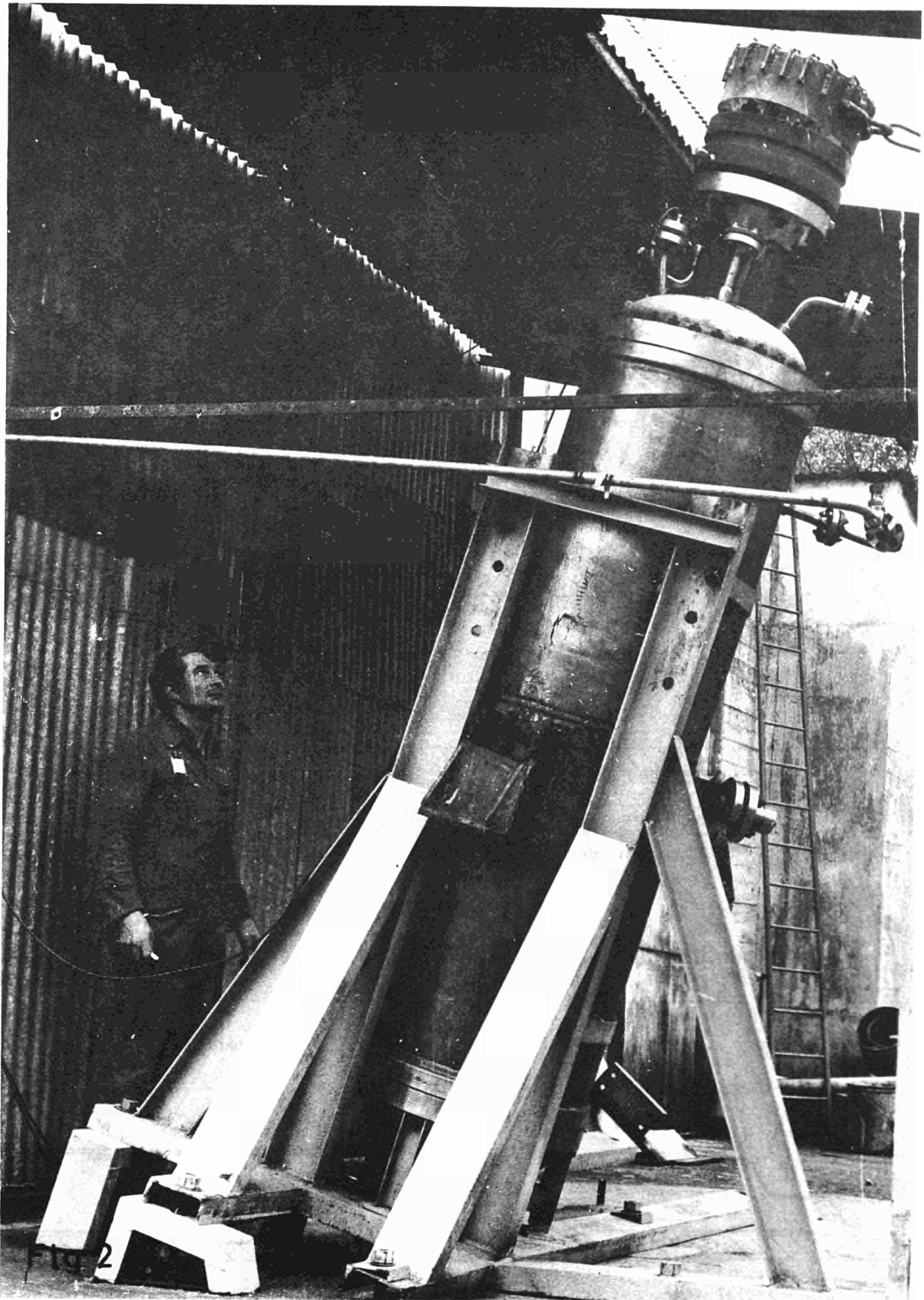
- Table 1 }
 - " 2 } - Numerical solutions of differential equation (23)
 - " 3 } - Experimental results
 - " 4 }
- " 5 - Results of tests C-5 and D-4
- " 6 - Results of permeability tests bobbin "3"
- " 7 - " " " " "4"
- " 8 - Metrology
- " 9 - Leak test

Facility for depressurisation tests on HTGR type insulations



Scale 1:12⁵

FIG. 1



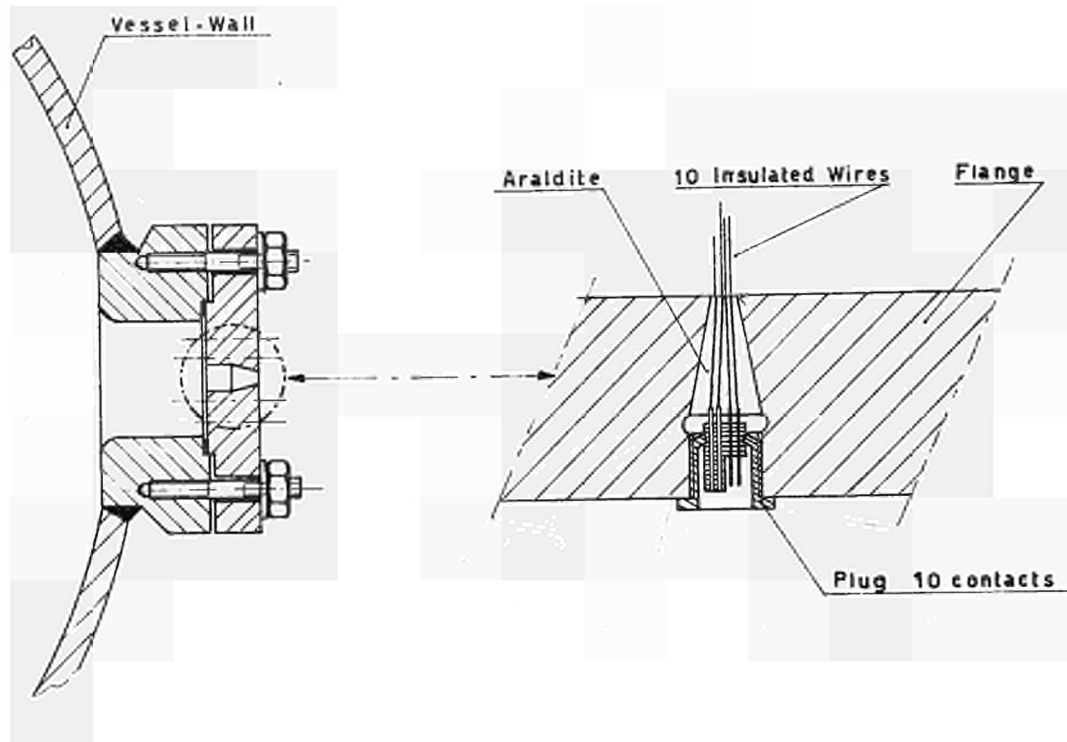
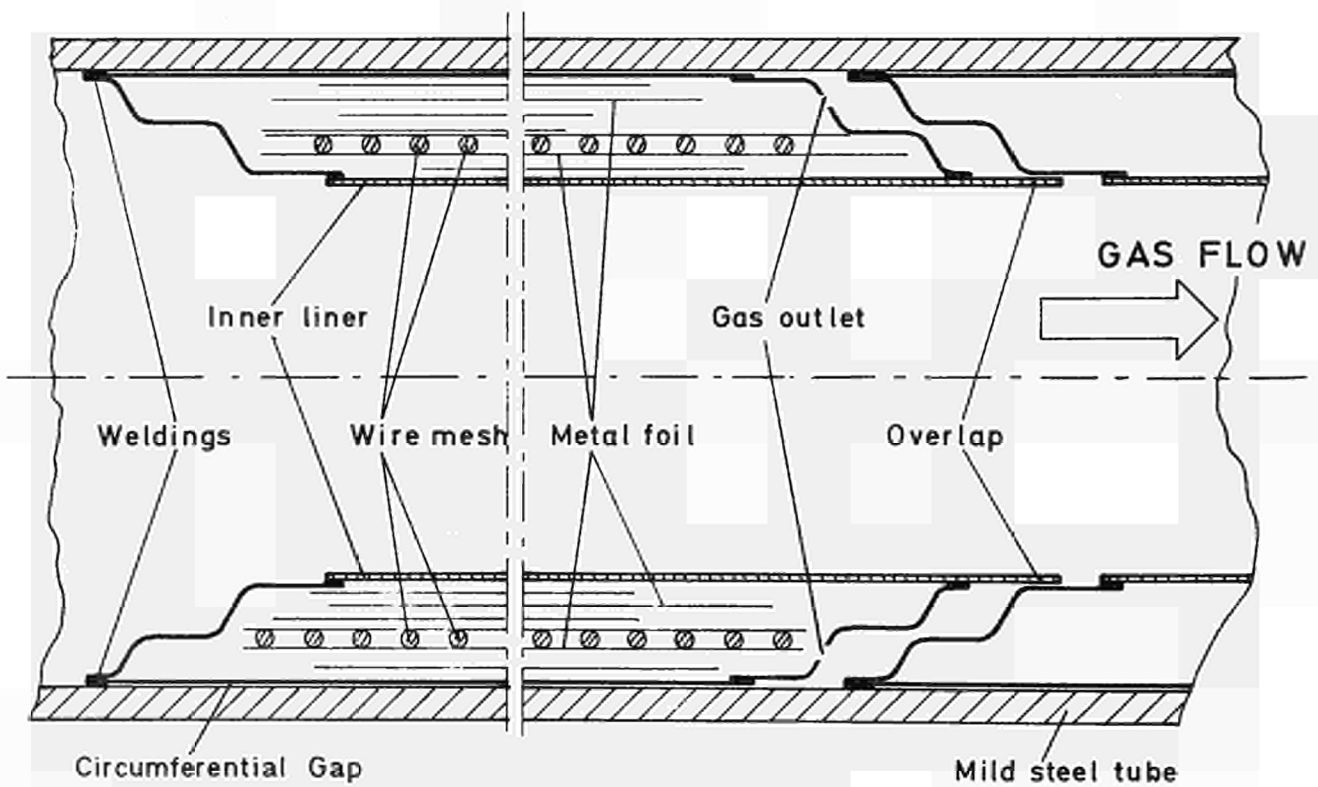


Fig. 3

Leak-tight Cable Outlet 50 Contacts.



SCHEMA OF INSULATION BOBBIN

Fig. 4

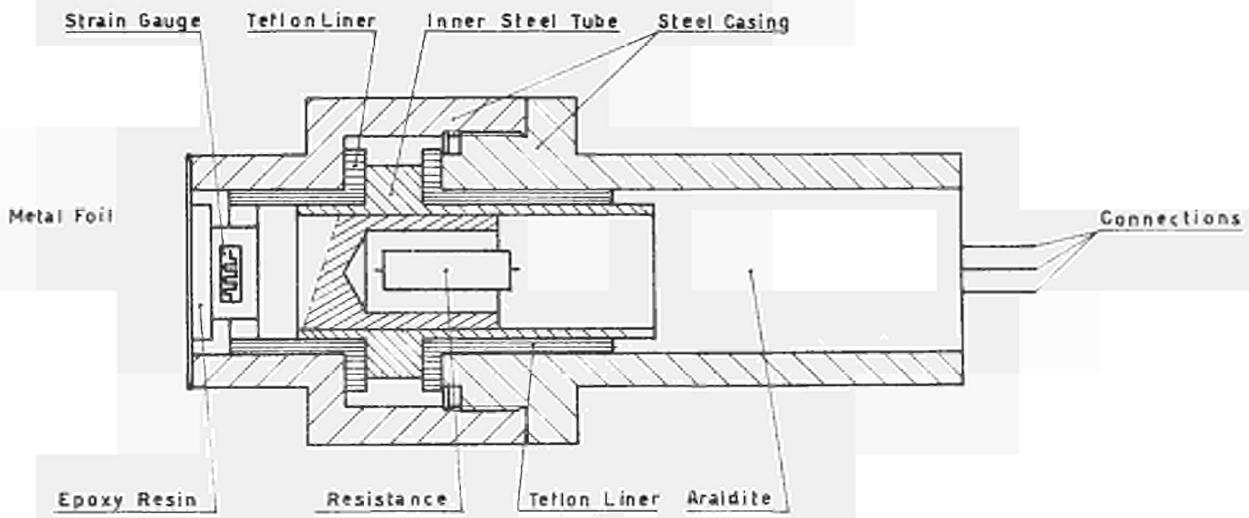


Fig. 5

Scale: 4:1

Cross-Section of Pressure Transducer (absolute)

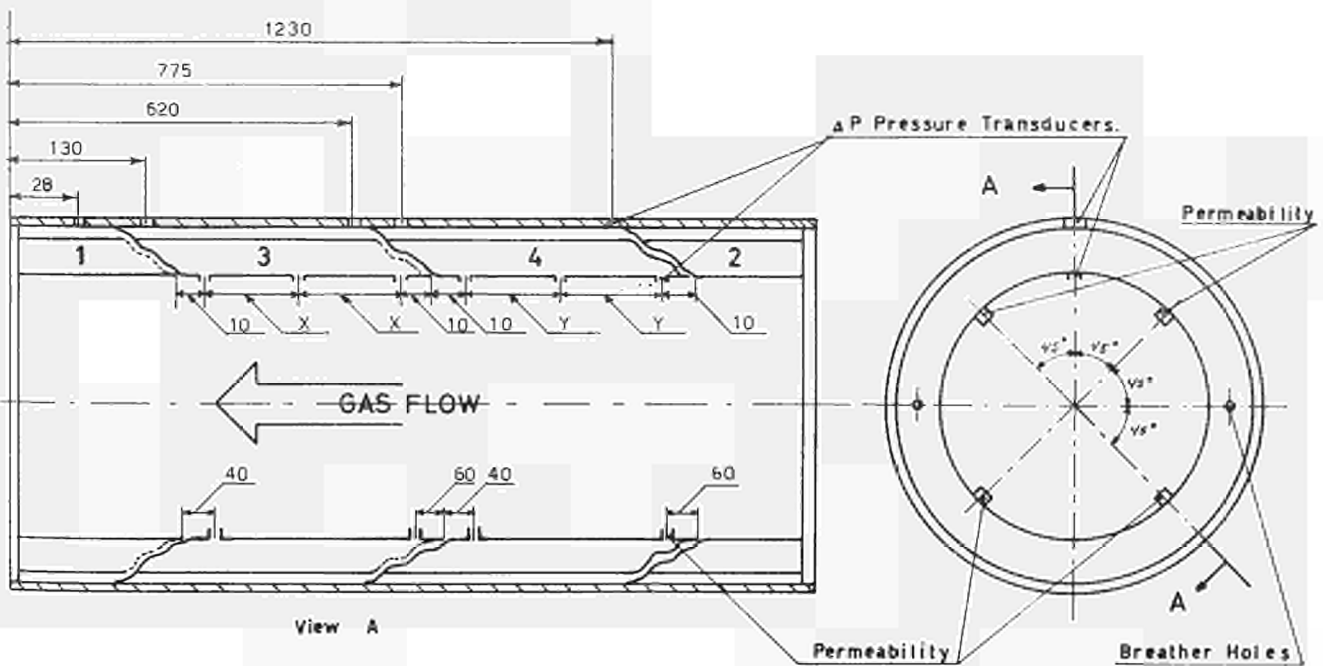
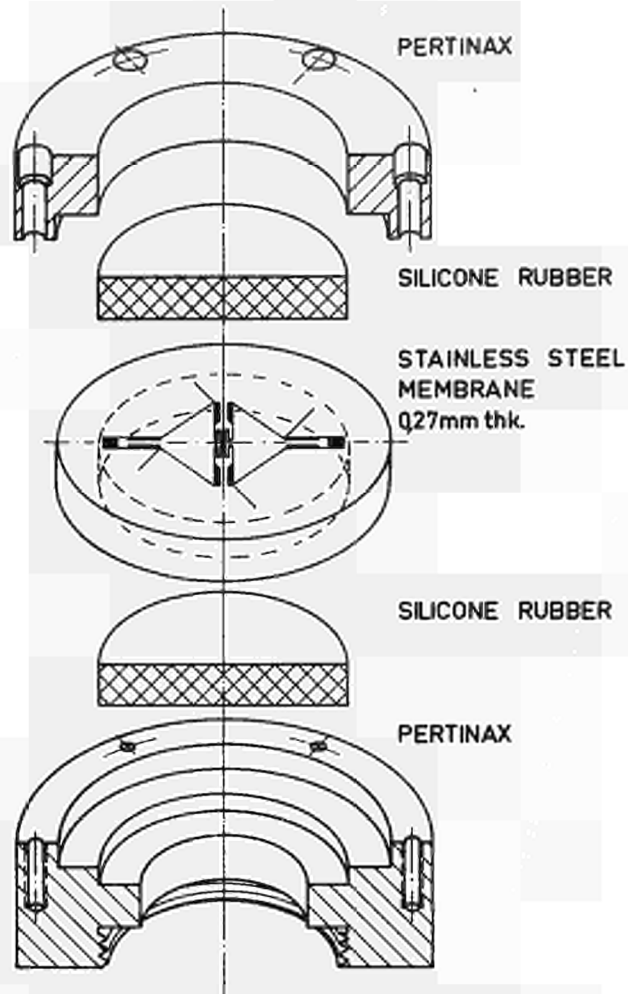


Fig. 6

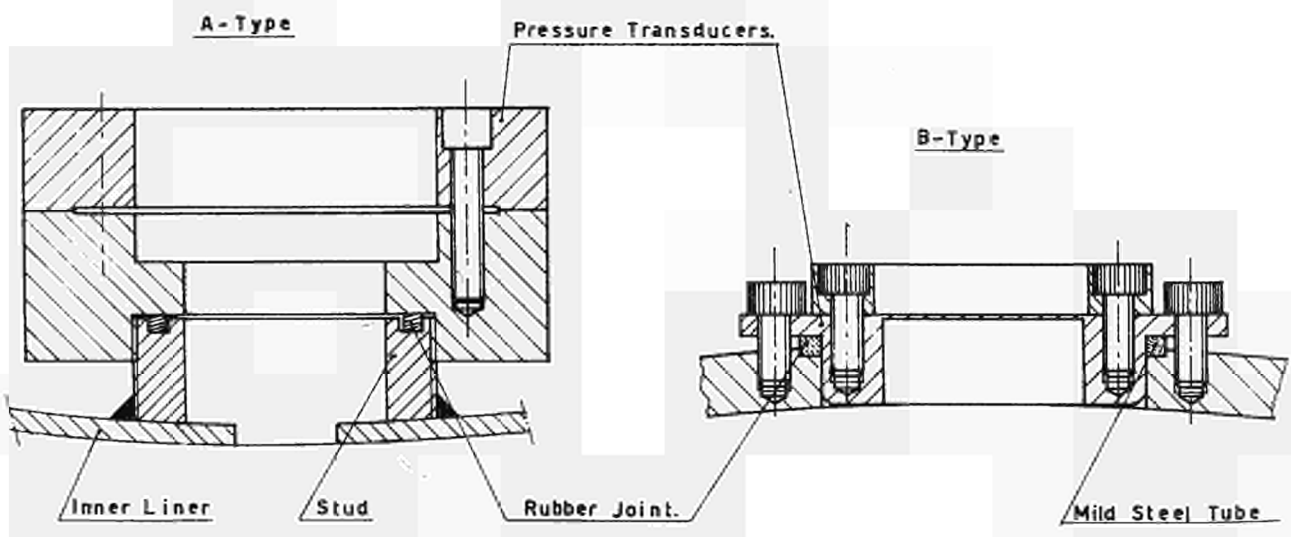
Mounting points for ΔP and Permeability measurements



DIFFERENTIAL PRESSURE TRANSDUCER

Fig. 7

(a-type)



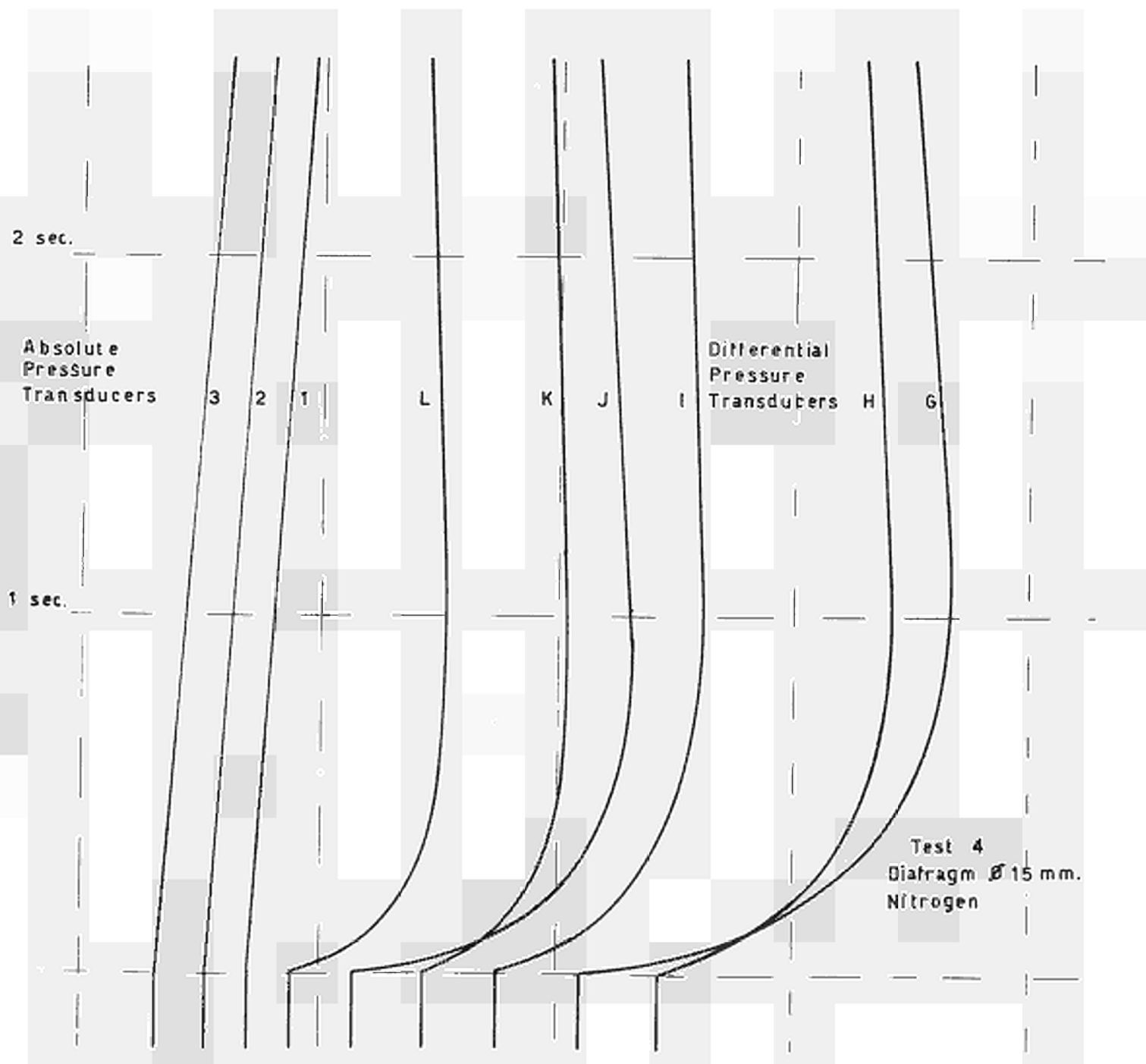
Scale: 2:1

Fig. 8

Differential Pressure Transducers.
Mounting on Bobbin (schematic)

Fig. 9

Example of enregistered curves



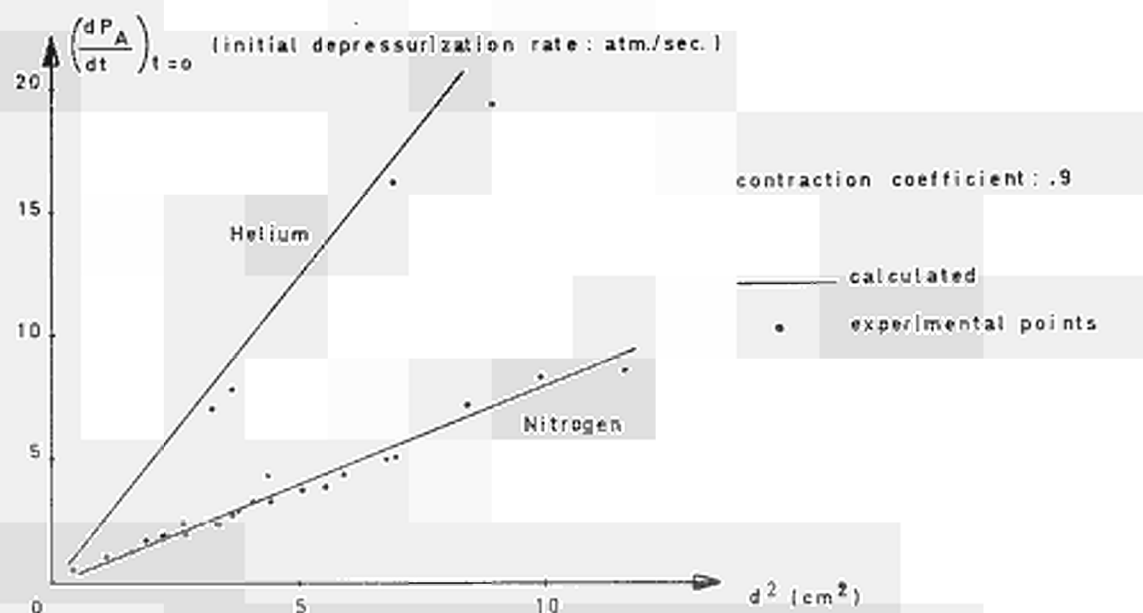


Fig. 10

DEPRESSURIZATION RATES VERSUS DIAPHRAGM
DIAMETER SQUARE

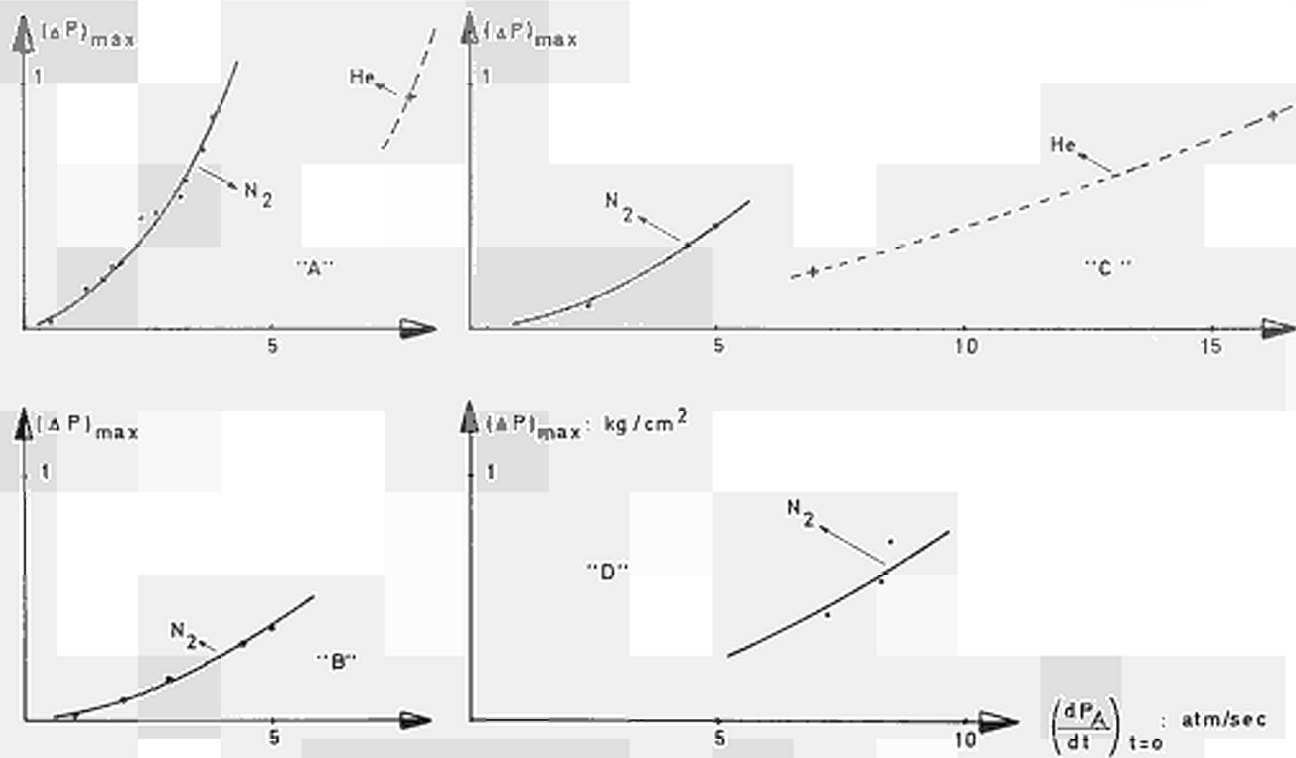


Fig. 11

EXPERIMENTAL RESULTS BOBBIN "3"

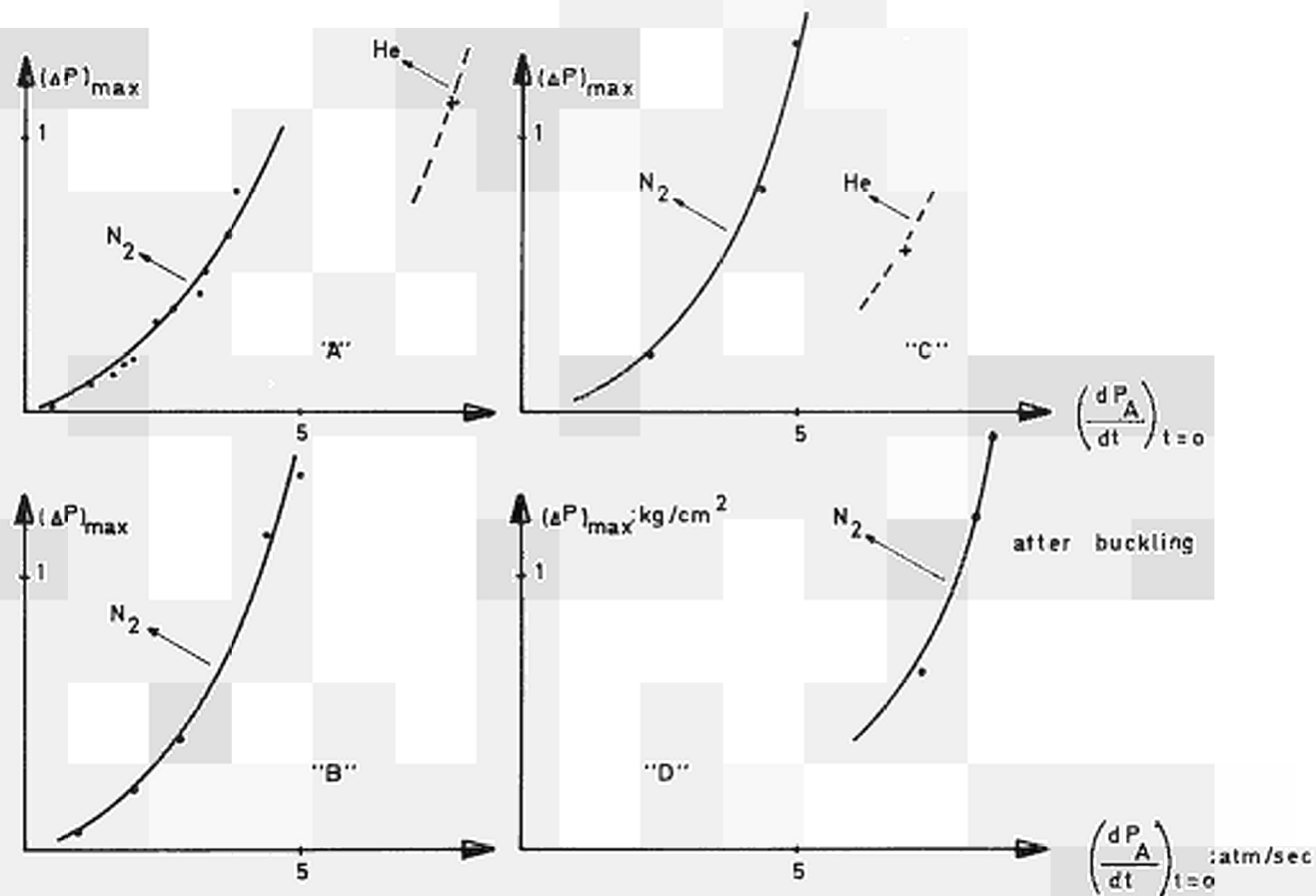
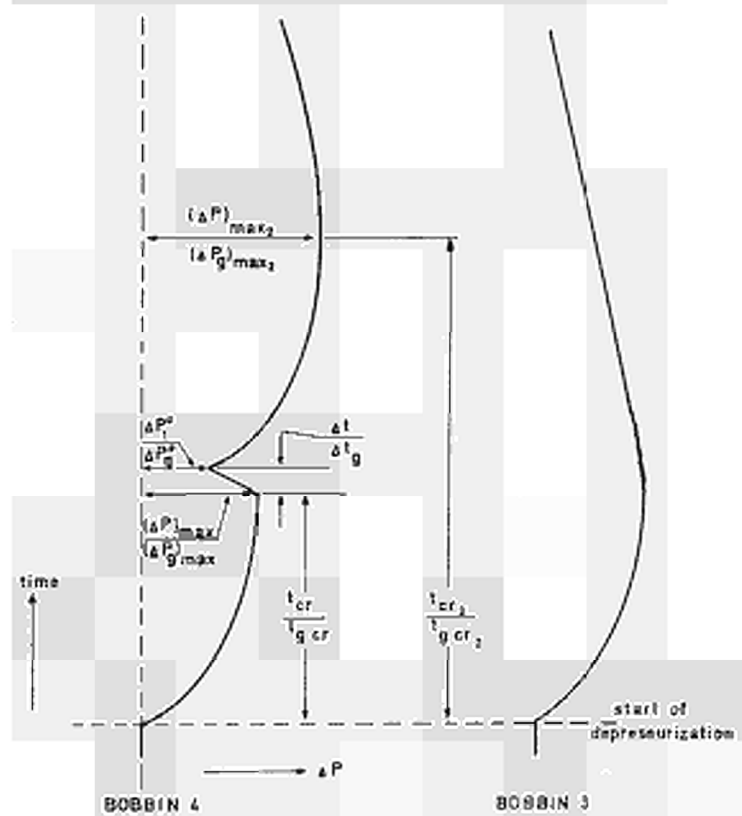


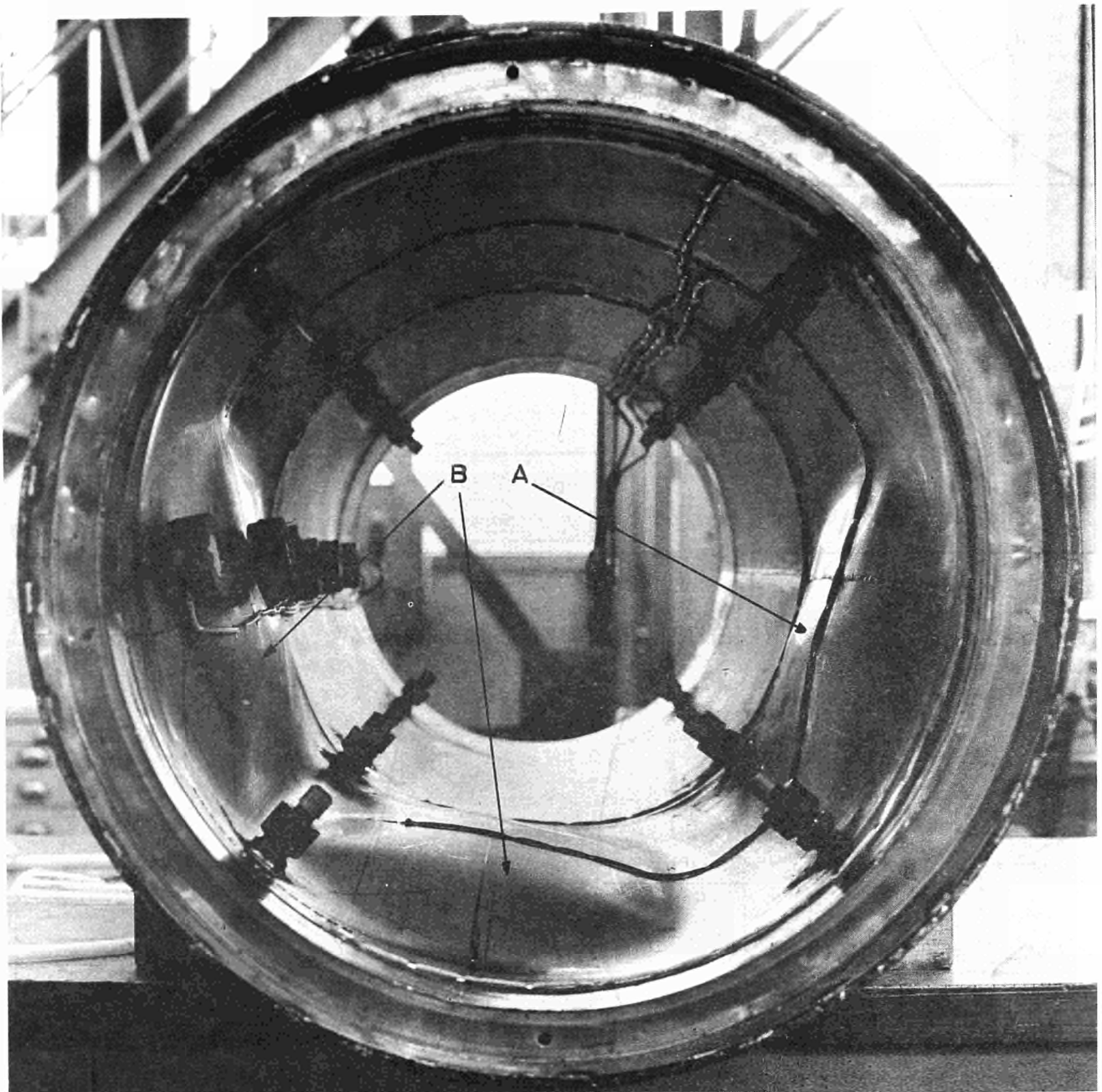
Fig. 12

EXPERIMENTAL RESULTS BOBBIN "4"



EXAMPLE OF RECORDING BUCKLING

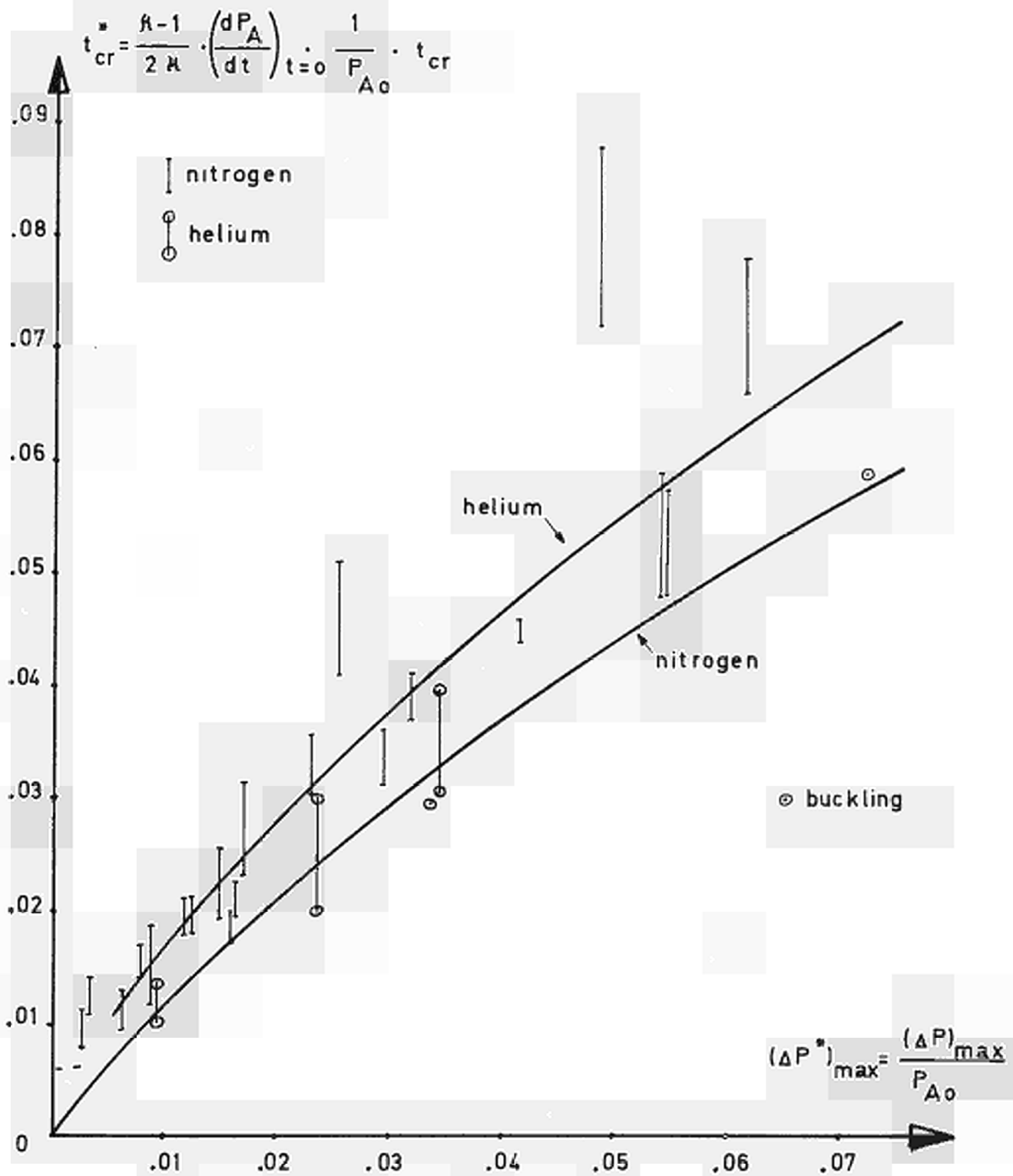
Fig. 13



A = first buckling
B = second buckling

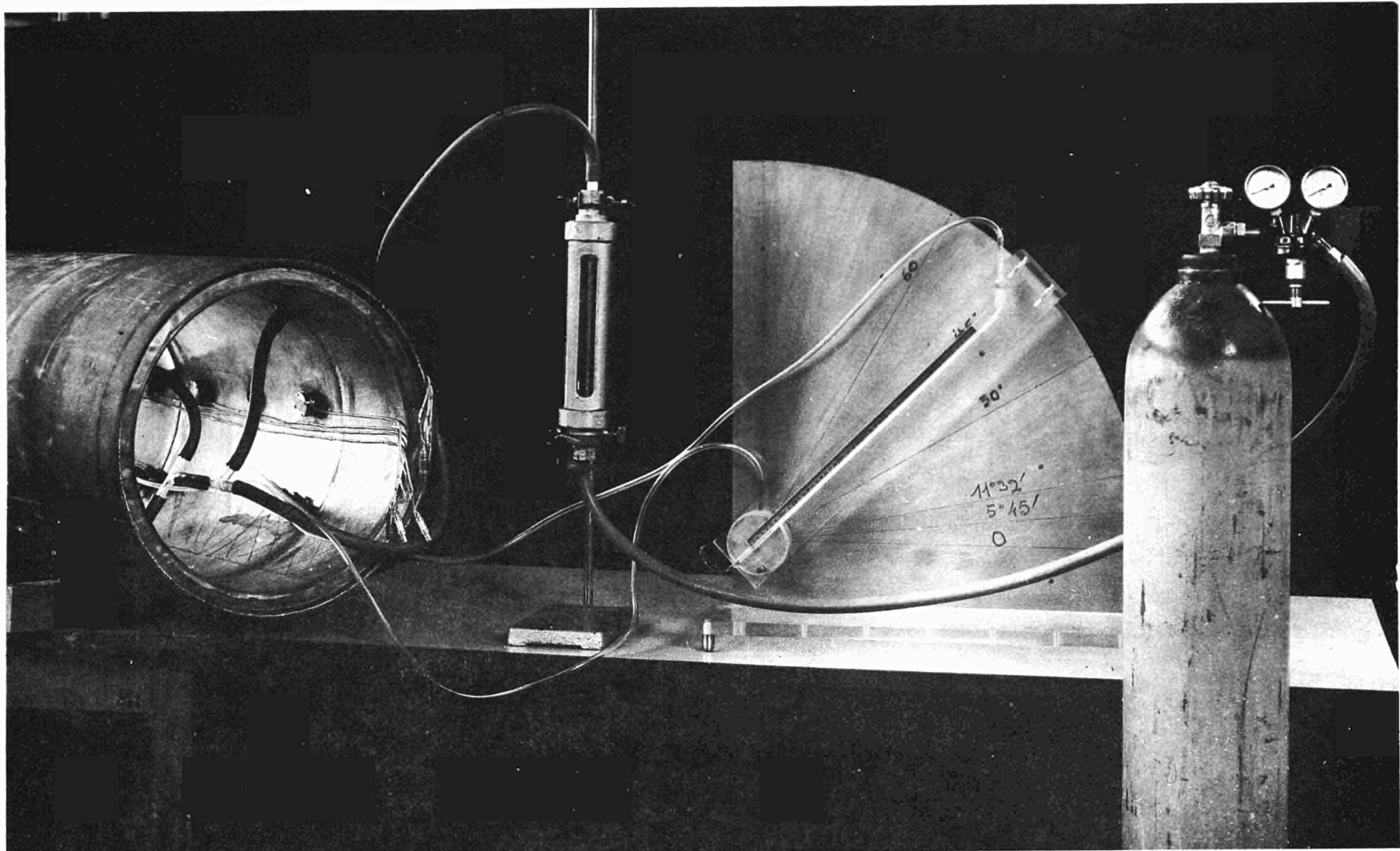
BOBBIN AFTER BUCKLING

Fig. 14



COMPARISON BETWEEN EXPERIMENTAL
AND THEORETICAL RESULTS

Fig. 15



TEST SET-UP FOR PERMEABILITY MEASUREMENT

Fig.16

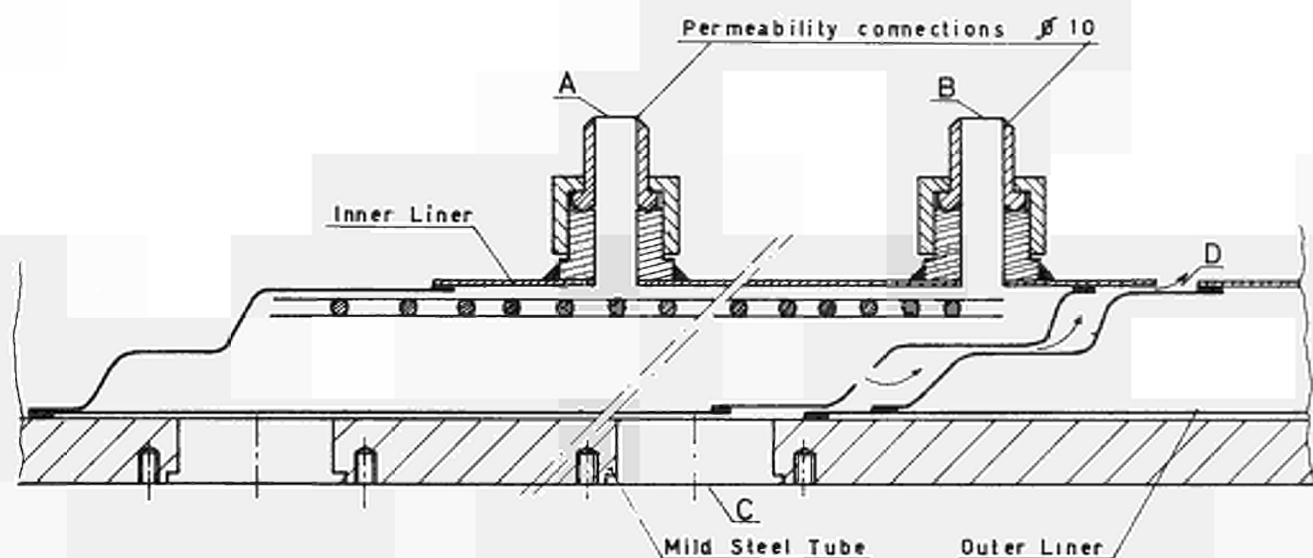


Fig. 17

Permeability Connections
Mounting on Bobbin (Schematic)

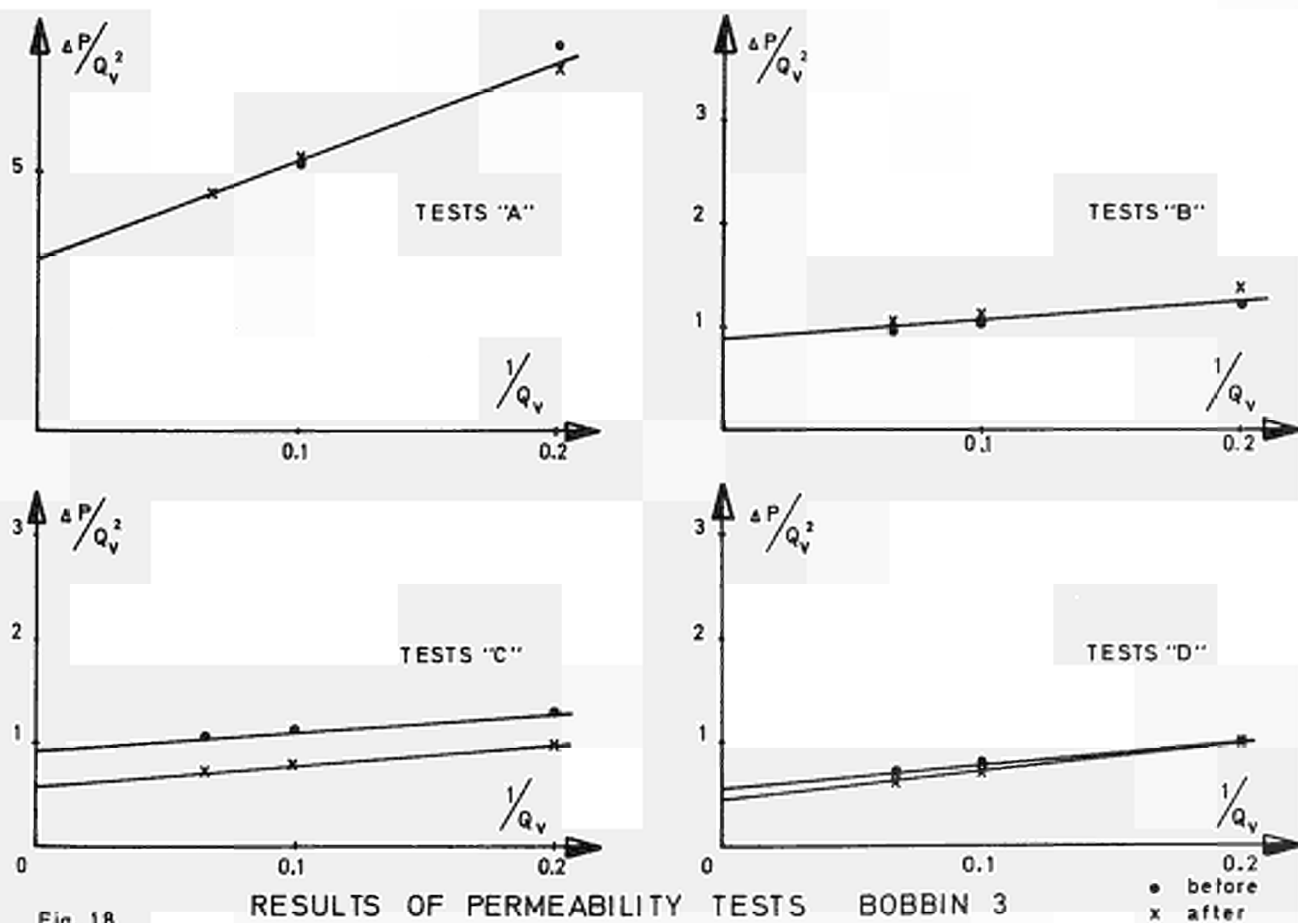
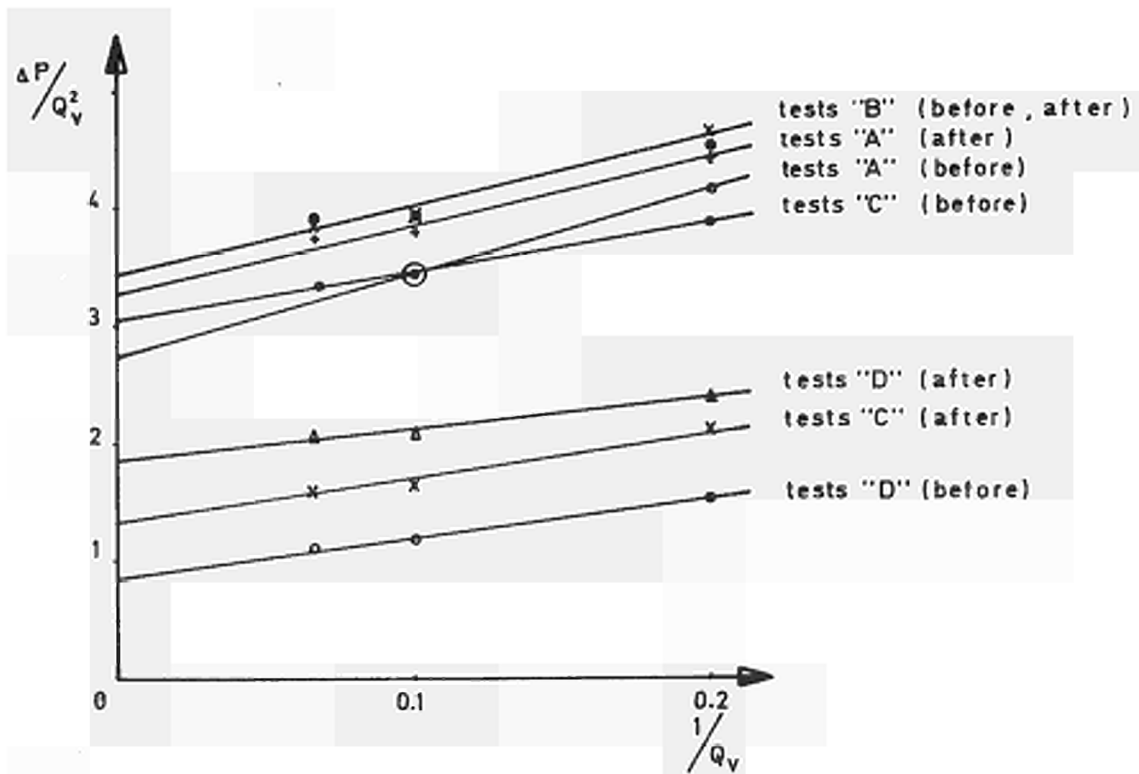


Fig. 18



RESULTS OF PERMEABILITY TESTS BOBBIN 4

Fig. 19

MEASURING POINTS METROLOGY AND POSITION OF X-RAY PHOTOGRAPHS

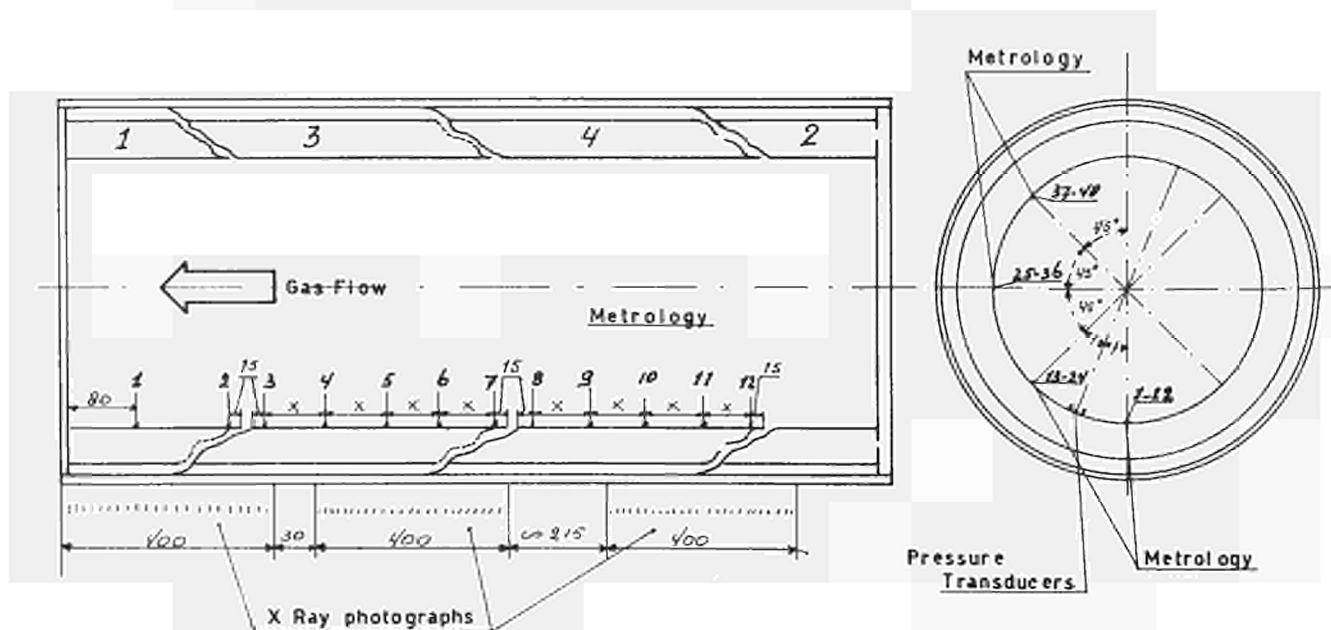
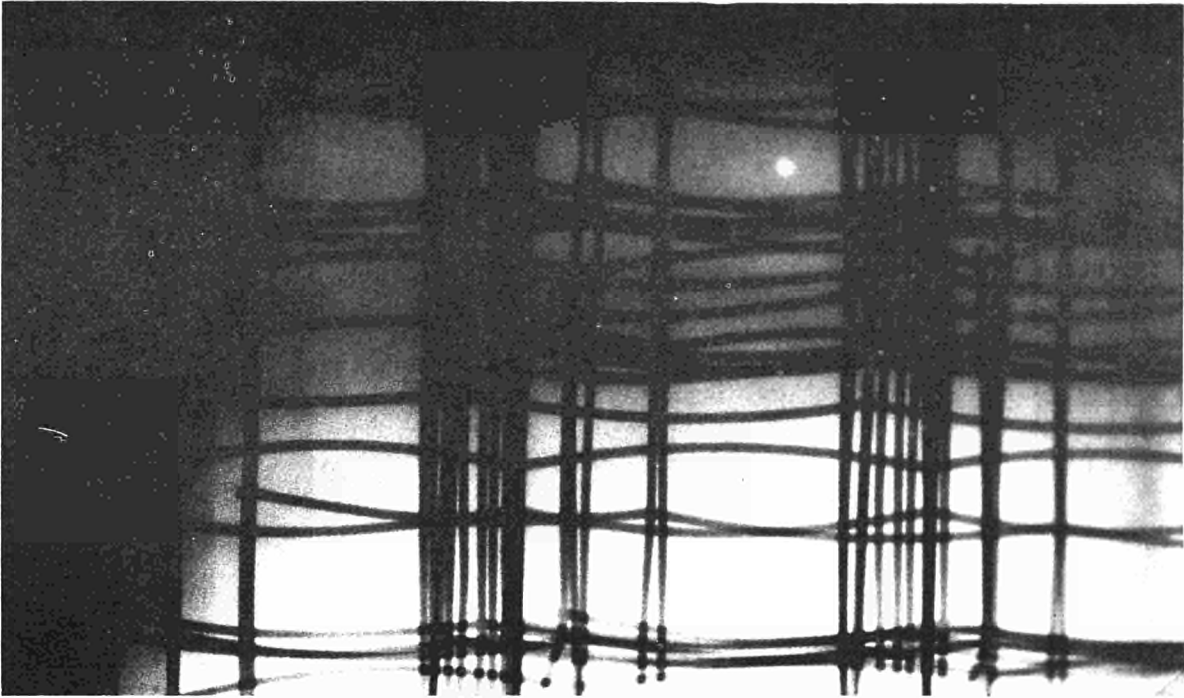
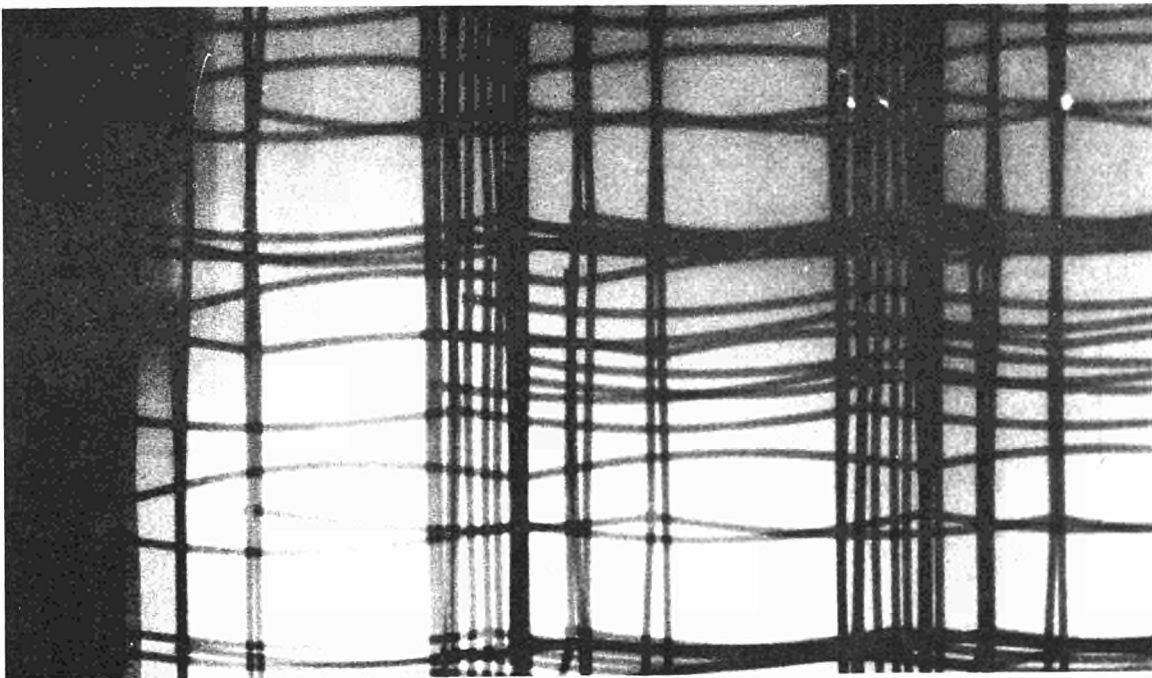


Fig. 20

Before depressurisation.

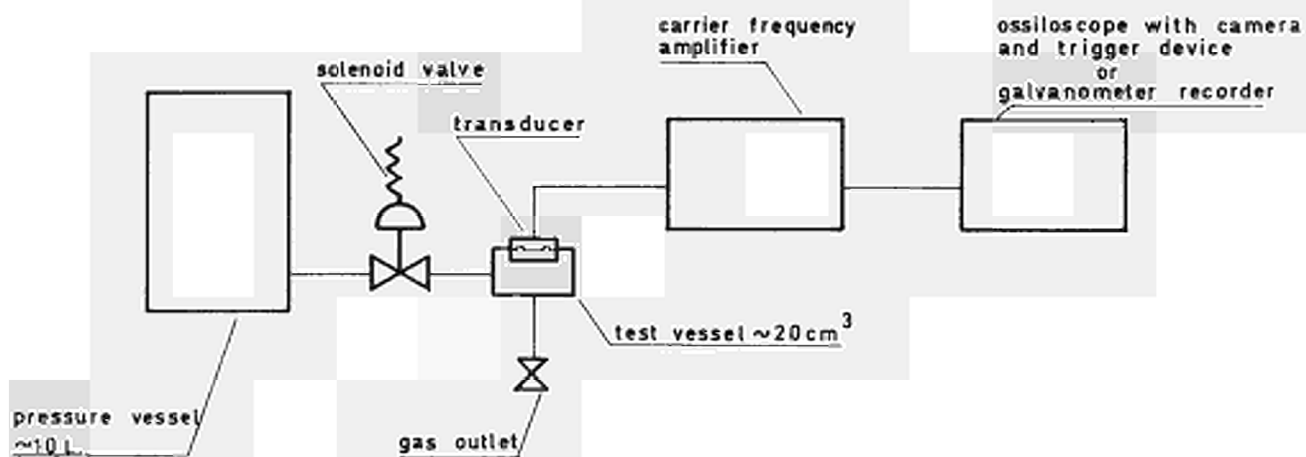
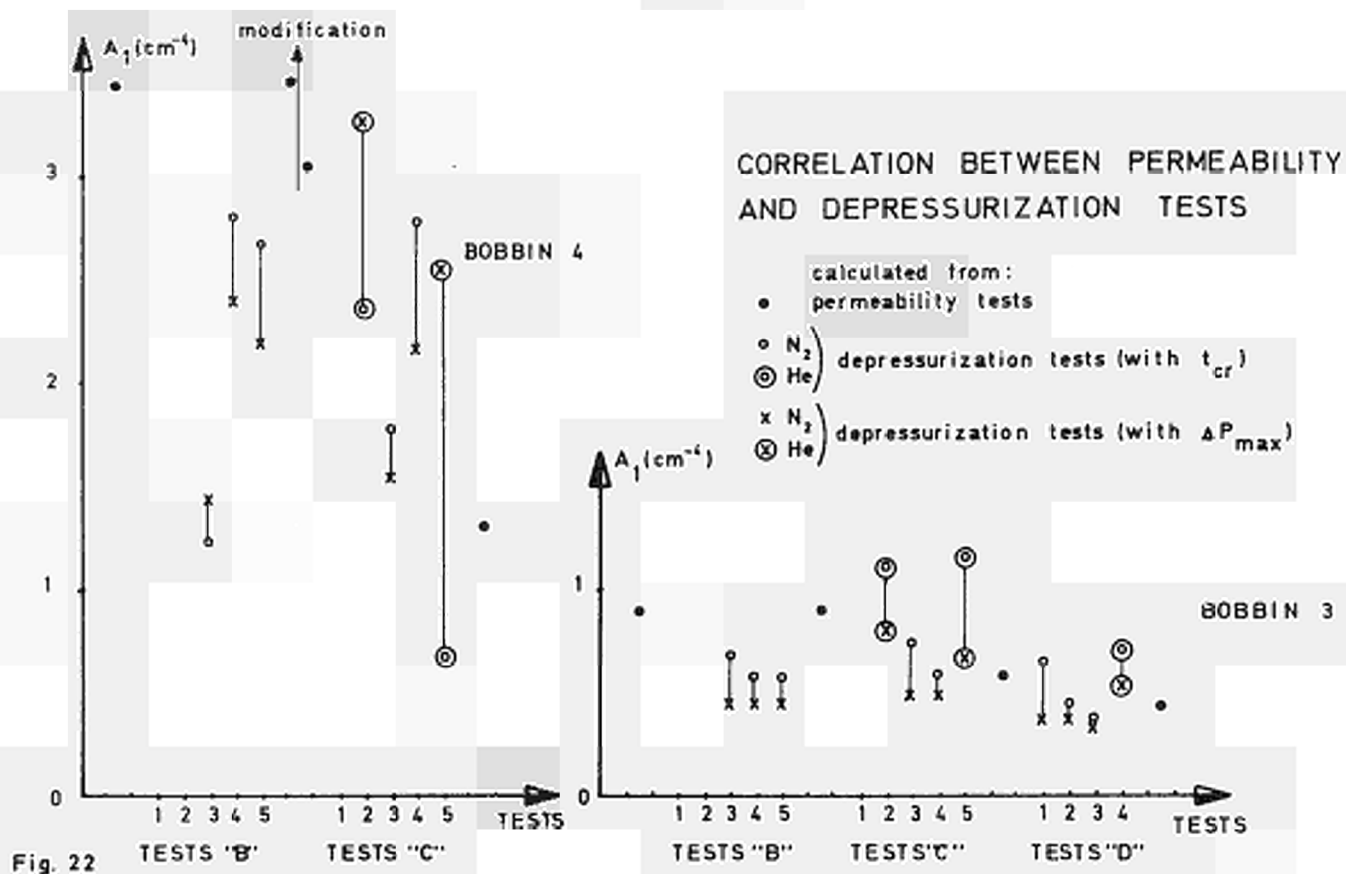


After depressurisation.



X Ray photographs.

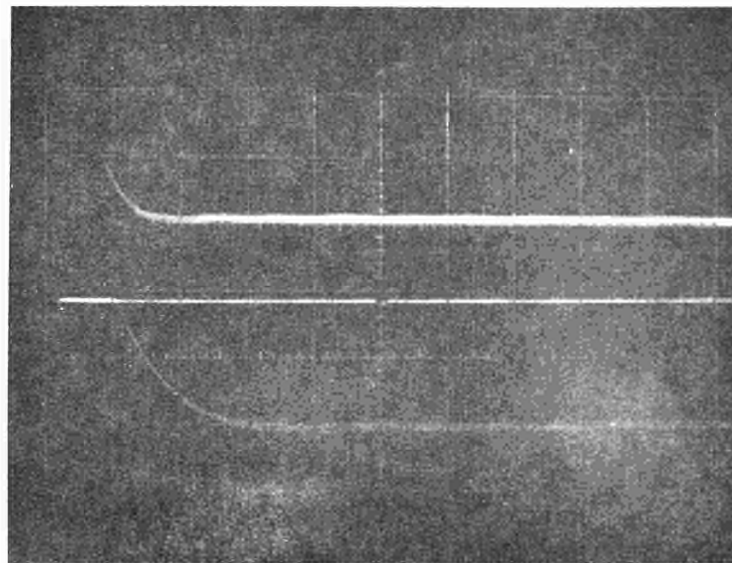
Fig.21



TEST SETUP FOR DIFFERENTIAL PRESSURE TRANSDUCERS (schematic)

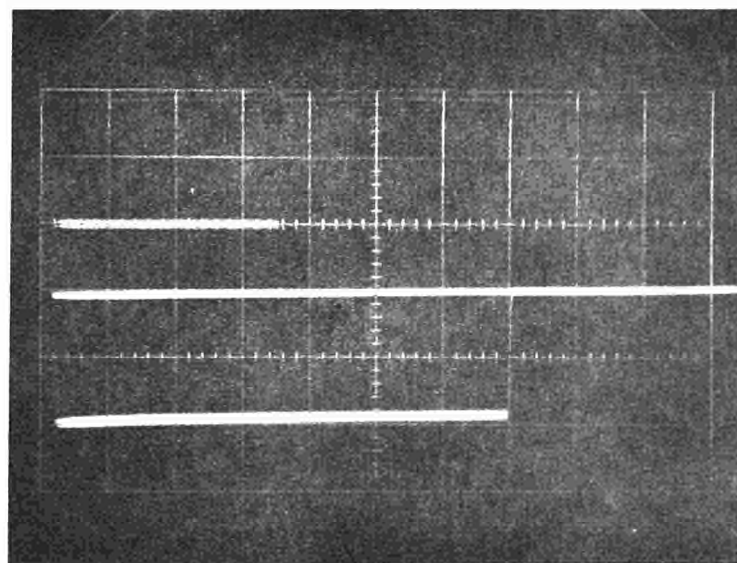
Fig. 23

↓
pressure
2 atm.



→ 20 milli sec./division (upper scale)
10 " " " (lower ")

↓
pressur
2 atm



→ 1 sec./division (upper scale)
0.5 " " (lower ")

PHOTOS OF DYNAMIC PRESSURE RECORDING

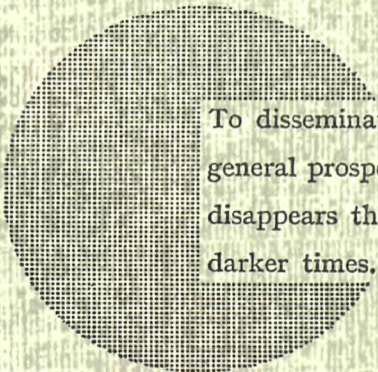
Fig. 24



NOTICE TO THE READER

All scientific and technical reports published by the Commission of the European Communities are announced in the monthly periodical "euro-abstracts". For subscription (1 year: B.Fr. 1 025,—) or free specimen copies please write to:

Office for Official Publications
of the European Communities
Case postale 1003
Luxembourg 1
(Grand-Duchy of Luxembourg)



To disseminate knowledge is to disseminate prosperity — I mean general prosperity and not individual riches — and with prosperity disappears the greater part of the evil which is our heritage from darker times.

Alfred Nobel

SALES OFFICES

The Office for Official Publications sells all documents published by the Commission of the European Communities at the addresses listed below, at the price given on cover. When ordering, specify clearly the exact reference and the title of the document.

GREAT BRITAIN AND THE COMMONWEALTH

H.M. Stationery Office
P.O. Box 569
London S.E. 1

UNITED STATES OF AMERICA

European Community Information Service
2100 M Street, N.W.
Suite 707
Washington, D.C. 20 037

BELGIUM

Moniteur belge — Belgisch Staatsblad
Rue de Louvain 40-42 — Leuvenseweg 40-42
1000 Bruxelles — 1000 Brussel — Tel. 12 00 26
CCP 50-80 — Postgiro 50-80

Agency:
Librairie européenne — Europese Boekhandel
Rue de la Loi 244 — Wetstraat 244
1040 Bruxelles — 1040 Brussel

GRAND DUCHY OF LUXEMBOURG

*Office for official publications
of the European Communities*
Case postale 1003 — Luxembourg 1
and 29, rue Aldringen, Library
Tel. 4 79 41 — CCP 191-90
Compte courant bancaire: BIL 8-109/6003/200

FRANCE

*Service de vente en France des publications
des Communautés européennes*
26, rue Desaix
75 Paris-15^e — Tel. (1) 306.5100
CCP Paris 23-96

GERMANY (FR)

Verlag Bundesanzeiger
5 Köln 1 — Postfach 108 006
Tel. (0221) 21 03 48
Telex: Anzeiger Bonn 08 882 595
Postscheckkonto 834 00 Köln

ITALY

Libreria dello Stato
Piazza G. Verdi 10
00198 Roma — Tel. (6) 85 09
CCP 1/2640

Agencies:
00187 Roma — Via del Tritone 61/A e 61/B
00187 Roma — Via XX Settembre (Palazzo
Ministero delle finanze)
20121 Milano — Galleria Vittorio Emanuele 3
80121 Napoli — Via Chiaia 5
50129 Firenze — Via Cavour 46/R
16121 Genova — Via XII Ottobre 172
40125 Bologna — Strada Maggiore 23/A

NETHERLANDS

Staatsdrukkerij- en uitgeverijbedrijf
Christoffel Plantijnstraat
's-Gravenhage — Tel. (070) 81 45 11
Giro 425 300

IRELAND

Stationery Office
Beggars' Bush
Dublin 4

SWITZERLAND

Librairie Payot
6, rue Grenus
1211 Genève
CCP 12-236 Genève

SWEDEN

Librairie C.E. Fritze
2, Fredsgatan
Stockholm 16
Post Giro 193, Bank Giro 73/4015

SPAIN

Librería Mundi-Prensa
Castello, 37
Madrid 1

OTHER COUNTRIES

*Sales Office for official publications
of the European Communities*
Case postale 1003 — Luxembourg 1
Tel. 4 79 41 — CCP 191-90
Compte courant bancaire: BIL 8-109/6003/200